Instrument identification to improve OR scheduling

Evaluating an RFID-based approach

J. Koffeman

Technische Universiteit Delft

TU Delft

Instrument identification to improve OR scheduling

Evaluating an RFID-based approach

by

J. Koffeman

to obtain the degree of Master of Science
at the Delft University of Technology,
to be defended publicly on Tuesday March 12, 2019 at 13:30.

Supervisor:	dr. J.J. van den Dobbelsteen	
	drs. F.C. Meeuwsen MD.	
Thesis committee:	dr. J.J. van den Dobbelsteen	TU Delft
	drs. F.C. Meeuwsen MD.	TU Delft
	P.E.A. Hermsen MSc.	TU Delft
	dr. M. van der Elst	RdGG

An electronic version of this thesis is available at `http://repository.tudelft.nl/`.

TU Delft

Contents

List of Abbreviations

The following abbreviations are used throughout this thesis:

CAD Computer-aided Design

CSSD Central sterile services department

DSMH Deskundige Steriele Medische Hulpmiddelen

EMI Electromagnetic interference

FDA Food and drug administration

IGJ Inspectie Gezondheidszorg en Jeugd

METC Medische Ethische Toetsingscommissie

OR Operating Room

RdGG Reinier de Graaf Gasthuis

RF Radiofrequency

RFID Radiofrequency Identification

TEP Total Extraperitoneal Laparoscopic Hernia Repair

TUD Technische Universiteit Delft

UHF Ultra high frequencies

WMO Wet medisch-wetenschappelijk onderzoek met mensen

List of Figures

List of Tables

Abstract

Hospitals are under an increased financial pressure, due to a significant growth in demand for healthcare, that is caused by an aging population. The operating rooms account for the largest costs of a hospital, and thus require a cost-efficient management. However, scheduling the operating rooms is a complex task that involves the estimation of surgery duration, which is often inaccurate. Delays in surgery duration, that are not accounted for in the estimation during scheduling, often result in upcoming surgeries being cancelled. Hence, the operating theatres are most of the time not fully utilized, which comes with great costs for the hospital. Poor communication of information about the progress of ongoing surgeries to the operating room (OR) schedulers prevents them from effectively (re)-scheduling accordingly. The OR personnel can not be assigned to additional tasks, and thus, there is a need for automated monitoring of the progress of ongoing surgeries. The instrument usage during surgeries is shown to provide relevant information about the progress of surgeries, using a Random Forest model to estimate surgical phases from intra-operative data.

In this thesis, a Radiofrequency Identification (RFID) setup is used to detect instruments, equipped with RFID-tags, that are used by the surgeon during a Total Extraperitoneal Laparoscopic Hernia Repair (TEP) procedure at Reinier de Graaf Gasthuis (RdGG). The setup is evaluated on applicability into a surgical setting, which involves regulatory aspects, acceptance by the OR-personnel, and performance. A pilot study, of which the results are incorporated into realizing actual in-vivo tests, is performed in a near-surgical setting to evaluate the extent to which the RFID-setup is applicable in a real surgical setting. During the pilot study, a total of 10 procedures is mimicked of which the data, that is extracted from the RFID-setup, is used to generate a Random Forest model that can estimate the surgical phases. The Random Forest model is used to evaluate the performance of the RFID-setup. After complying with all regulations to perform in-vivo testing, a total of three in-vivo tests is executed to evaluate the applicability of the RFID-setup in a real surgical setting. Lastly, a first step has been taken to extend the research to a greater range of surgery types.

The RFID-setup has shown the ability to identify instruments, that are equipped with RFID-tags, during surgery. All regulations to perform in-vivo tests are complied with, and no discomfort of the RFID-setup is experienced by the OR-personnel during the in-vivo tests. Hence, future in-vivo testing is warranted to optimize the setup. The Random Forest model can estimate the phases of surgeries (38% overall accuracy), based on instrument usage data that is acquired through an RFID-setup. The current setup, however, needs to be optimized to improve the detection ability. So far, the first step to make the method of instrument identification applicable to a broader range of surgeries has resulted in a prototyped attachment design to equip instruments with RFID-tags. The attachment is designed in such a way that both the attachment and the RFID-tags are interchangeable between instruments. Further development is needed for the design to comply with a selection of regulations to perform in-vivo testing.

1 Introduction

1.1. Operating room scheduling

Hospitals are under an increased financial pressure, due to a significant growth in demand for healthcare that is caused by an aging population [4]. The operating rooms account for the largest costs of a hospital [5], and thus require a cost-efficient management, while achieving a high quality of care. However, managing the operating rooms is a complex task that involves scarcity of resources [4] and staff. Also, the Operating Room (OR) scheduling is often inefficient due to inaccurate predictions of surgery duration [6], which are based on pre-operative consultations that do not account for variability in patient parameters [7]. With OR-scheduling being inefficient most of the time, theatres are not fully utilized [8], which is very costly for the hospital. Moreover, delayed surgeries often result in the cancellation of upcoming surgeries, which causes significant inconvenience to the already stressed patients [9]. A complete process that a patient goes through is divided into three stages: preoperative stage, which involves patient preparation; intraoperative stage, which involves the actual surgery; and the postoperative stage, where the patient is prepared for discharge [10]. This study focuses on the intraoperative stage, and more specifically, on the actual surgery. Uncertainties in surgery duration are mainly due to unpredictable events (e.g. equipment malfunctioning) and complications during surgeries. Information on the progress of the surgery is often poorly communicated with the OR-schedulers. Since OR-schedulers are not able to visually keep track of all ongoing surgeries, and additional phone-calls disrupt the work of the OR-staff [7], the OR-schedules are difficult to be efficiently adapted throughout the day. The OR-personnel can not be assigned to additional tasks, as their workload is already significant and thus, there is a need for automated monitoring of the progress of ongoing surgeries.

1.2. Surgical workflow recognition

An increased interest is developing towards surgical workflow recognition, where the term workflow is considered to describe a surgical process or intervention [11]. The aim of surgical workflow recognition is to automatically monitor the progress of surgeries, which can provide essential information to optimize OR-occupation and staff scheduling [12]. In the area of surgical workflow recognition, several methods are researched. The literature shows workflow analyses by means of location aware systems to monitor the movement of the surgical staff [13], eye-tracking [14], and intra-operative data such as suction bag weights, intra-abdominal CO_2 pressure and the inclination of the surgical table [15]. Another aspect of surgical workflow recognition, which is researched most popularly [2], is the segmentation of the surgical workflow based on identification of instruments that are used during surgeries.

1.3. Instrument identification

The usage of numerous instruments, or combinations of instruments, points at specific surgical tasks. Once instruments can be identified based on unique numbers or instrument-types, segments of the surgical workflow can be distinguished automatically based on the usage information of these identified instruments. Instrument identification during surgeries has already repeatedly been studied in the context of minimally invasive surgeries, where the identification of instruments is based on the analysis of endoscopic or microscopic images [16]. However, the analysis of endoscopic or microscopic images is limited to minimally invasive

surgeries and thus, poorly applicable to a broader range of surgeries. A selection of studies showed instrument identification based on visual markers that are attached to the instruments [17] [18] [19]. The markers are either detected using the endoscopic images, which again limits the applicability to minimally invasive surgeries only; or by a camera system that is installed somewhere in the OR where the markers are visible to the camera. In general, camera systems are not likely to be accepted within the OR due to privacy reasons and consent issues. Furthermore, Meißner and Neumuth have presented promising results for instrument identification based on Radiofrequency Identification (RFID) [20]. RFID is a technique where data on tags is transferred to a reader by means of radio signals. The tags are identified based on their unique response. In case of instrument identification, the tags are attached to the instruments. Amongst alternative identification techniques which are still in an early stage of research, RFID-based identification is deemed to be the most suitable method for instrument identification during surgeries [21]. Although RFID-based identification of instruments has already been studied in lab-settings, limited studies are found that performed in-vivo tests using RFID-tags attached to instruments [22].

1.4. Surgical process recognition

Given that, theoretically speaking, data about the instrument usage can be acquired, it is shown that machine learning models can estimate the progress of the surgery from this data [2]. The estimation of the progress of the surgery can be described in different levels of abstraction, also called granularity [1]. The different levels of granularity are visualized in Figure 1.1, where the granularity increases from top to bottom. The surgical context increases from bottom to top. A surgical procedure can be divided into different phases, which are characterized by events or other factors such as instrument usage. Phases consist of steps that are composed of different activities. The activities are realized by the physical motions of the surgeon [1]. The highest level of granularity is the information that can be acquired using low-level sensory data (e.g. infrared camera images, or CO_2 pressure).

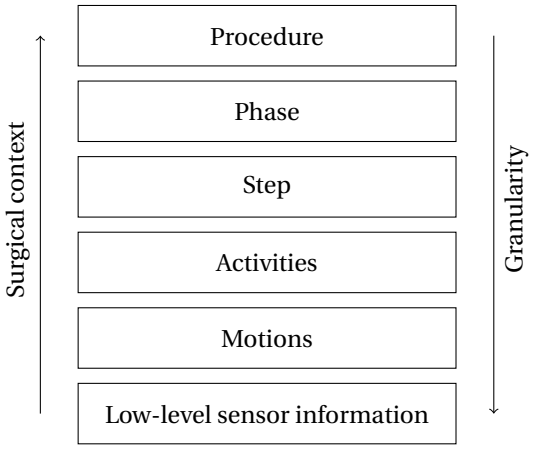

Figure 1.1: Different levels of granularity of a surgical procedure, adapted from [1] and [2].

The phases of a procedure are considered to be most suitable for tracking the progress of a surgical procedure [2]. Therefore, in this study, low-level sensor information is used as an input for a machine learning model to recognize surgical phases, see Figure 1.2. The low-level sensor information is acquired by means of an RFID-system, where RFID-tags are attached to the instruments during surgery.

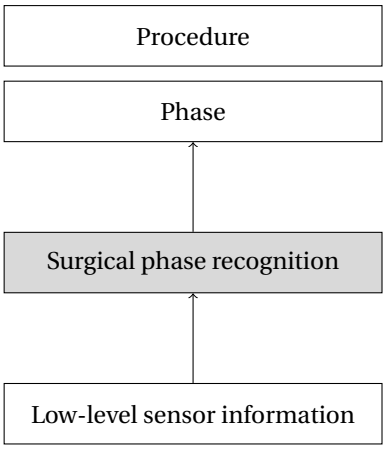

Figure 1.2: Surgical phase recognition reconstructs the phases, based on low-level sensor information, adapted from [2].

1.5. Problem statement and research question

The lack of information about the progress of ongoing surgeries that is provided to the OR-schedulers can be solved using surgical phase recognition models that estimate the progress of the surgery. However, there is still a gap between the actual surgery and these models, which needs to be bridged by intra-operative data. Therefore, the problem statement is as following:

Problem Statement

In order to improve the efficiency of operation room scheduling, a method is needed to acquire intra-operative data during surgeries, which can provide surgical process models with the necessary information to estimate the surgical progress.

Reinier de Graaf Gasthuis (RdGG), which is located in Delft and Voorburg, granted access to their operating rooms and Total Extraperitoneal Laparoscopic Hernia Repair (TEP) procedures during this research. TEP-procedures are common, and thus, a sufficient amount of data can be acquired within the timeframe of this study. The TEP-procedure is further elaborated in Section 1.7. Instrument identification can be applied in a surgical environment, providing low complex intra-operative data. Therefore, this thesis will focus on the implementation of RFID-technology to identify surgical instruments during surgery.

Research Question

To what extent is instrument identification using RFID-technology applicable into a surgical environment, without inferring with the surgical process?

The RFID-technology is already shown to accurately identify instruments [20]. However, the technology is not yet studied often in a surgical environment while aiming at surgical phase recognition. The overall method of instrument identification, using an RFID-setup, is yet to be accepted based on regulations and by the OR-personnel. Also, the performance of the RFID-setup must be evaluated. Lastly, within the timeframe of this study, only the TEP-procedures can be included in the research. Nevertheless, the method of instrument identification needs to be adaptable to a broader range of surgeries, in order for future research to evaluate the applicability of the researched method of instrument identification more comprehensively. Thus, the research goals can be stated as following:

Research Goals

1. Evaluate the acceptance by OR-personnel of an RFID-setup into a surgical environment.
2. Evaluate the regulatory acceptance of an RFID-setup into a surgical environment.
3. Evaluate the performance of an RFID-setup to identify surgical instruments.
4. Make the method of instrument identification applicable to a broader range of surgeries.

1.6. RFID-technology

Radiofrequency Identification (RFID) is a method of remotely reading data that is stored on RFID-tags, which are referred to as 'tags' from now on. RFID is already widely applied in the field of security and supply chain management [23]. A complete RFID-setup consists of an antenna, a reader, a computer with the software installed to communicate with the reader, and finally, tags to detect. The antenna transforms the electrical current from the reader to Radiofrequency (RF)-waves and emits those. The RF-waves activate the tags that are within the reading range of the antenna, which in turn backscatter the signal. The backscattered signals are received by the antenna and converted back to an electrical current, which is sent to the reader. The reader communicates this signal with the computer.

In general, a distinction can be made between active and passive tags. The main difference between active and passive tags is that active tags are powered by an internal power source, while the circuitry of passive tags is powered by the energy from the RF-waves. The reading range of active tags (up to 100m) is much higher than passive tags (up to 10m) since the internal power source enables the active tags to transmit stronger signals back to the antenna. However, the dimensions of active tags are significantly larger due to the presence of the internal power source, and active tags are much more expensive.

RFID operates under four different frequency ranges within the electromagnetic spectrum, as presented in Table 1.3. Besides the greater reading ranges, RFID-systems that operate in the Ultra high frequencies (UHF) range offer additional advantages over systems that operate within the Low Frequency- or High Frequency range. UHF systems are better capable of simultaneously reading multiple tags, and since the wavelength is shorter, the antennas can be smaller. However, the signal of UHF systems is more vulnerable to interference with surrounding materials like liquids or metals.

Figure 1.3: RFID operating frequencies [3].

Band	**LF Low frequency**	**HF High frequency**	**UHF Ultra high frequency**	**Microwave**
Frequency	30–300kHz	3–30MHz	300 MHz–3GHz	2–30 GHz
Typical RFID Frequencies	125–134 kHz	13.56 MHz	433 MHz or 865 – 956MHz 2.45 GHz	2.45 GHz
Approximate read range	less than 0.5 metre	Up to 1.5 metres	433 MHz = up to 100 metres 865-956 MHz = 0.5 to 5 metres	Up to 10m

1.7. TEP procedure

A Total Extraperitoneal Laparoscopic Hernia Repair (TEP) is one of the most common laparoscopic procedures to repair an inguinal hernia [24]. An inguinal hernia is an opening in the abdominal wall through which body tissue, or, mostly part of the intestines is protruded into a sack of protruded peritoneum [25]. In general, the surgeon retracts the inguinal hernia using laparoscopic tools which are inserted through keyholes in the abdomen. The opening in the abdominal wall through which the hernia was protruded is then covered with a mesh to strengthen the wall. Figure 1.4 shows the general position of relevant surgical equipment and personnel during a TEP procedure.

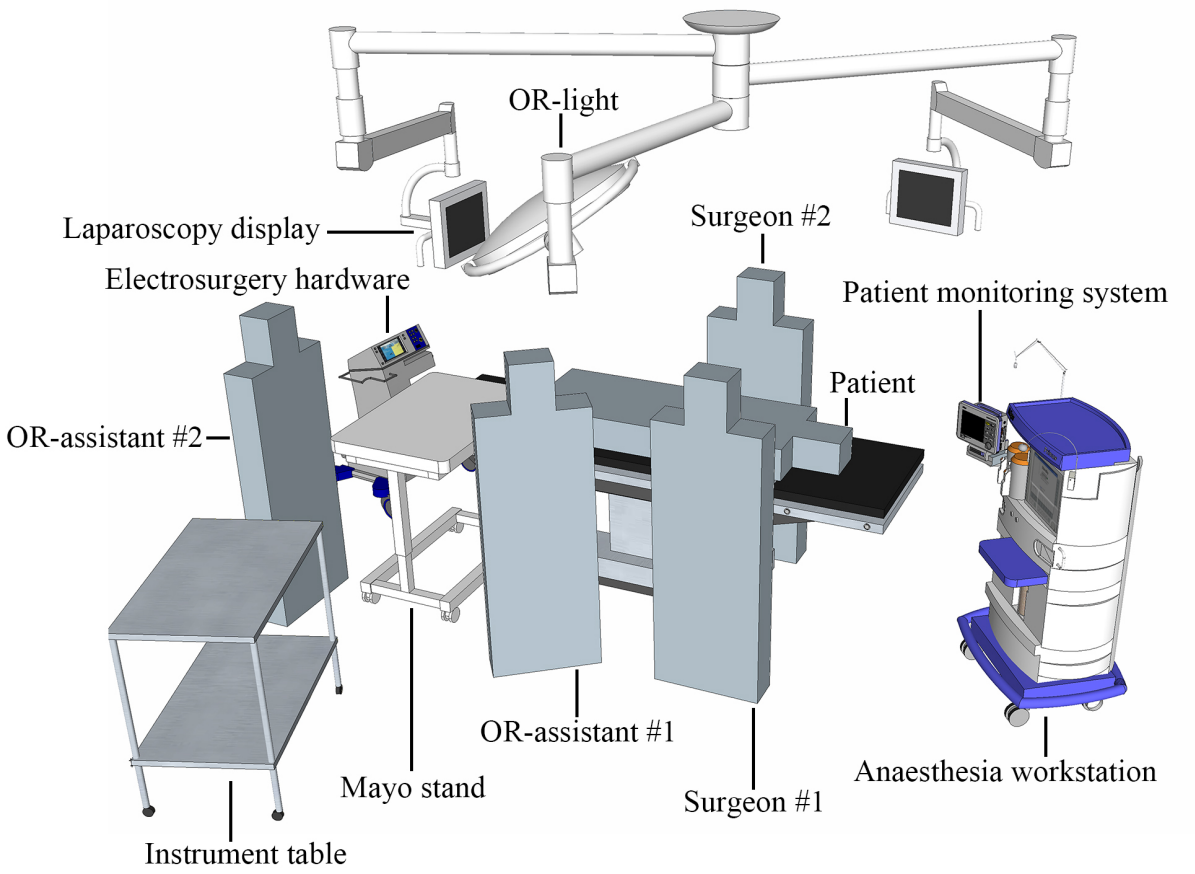

Figure 1.4: Position of relevant surgical equipment and personnel during a TEP procedure.

A TEP-procedure is divided into the following steps [26]:

1. Introduction first trocar (starts with horizontal subumbical incision).
2. Introduction second trocar.
3. Introduction third trocar (starts with the dissection to Bogros' space).
4. Identification of epigastric veins, os pubis, Cooper's ligament, funiculus/rotundum and hernial sac.
5. Identify hernia type (direct/indirect).
6. Reduction of the inguinal hernia.
7. Preparation and introduction of preperitoneal mesh.
8. Placement and fixation of preperitoneal mesh.
9. Wounds closure.

1.8. Outline

Figure 1.5 presents a gross overview of the two-folded research as presented in this thesis, where the rectangles refer to chapters, whereas rounded white rectangles refer to parts. After the introduction of the thesis, there is a split into two parts.

The first part describes the process of evaluating the applicability of RFID-technology into a surgical setting. This evaluation concerns the regulatory acceptance, the acceptance of the RFID-technology by OR-personnel, and the performance of the RFID-technology. A pilot study is performed to evaluate the performance and acceptance of the RFID-setup that was available at that moment. The results of the pilot study are incorporated into the process of realizing eventual in-vivo tests. After the pilot study, work is described on approvals that are obligated to perform an in-vivo test. Once all approvals were obtained, several in-vivo tests were performed to evaluate the applicability of the current RFID-setup in a real surgical setting. The second part of this thesis describes the process of designing an attachment to equip instruments with RFID-tags that allows for interchanging tags between instruments. The interchangeability of tags between instruments is necessary to extend the research as presented in this thesis to a broader range of surgeries. The second part of this thesis first introduces the current problem, followed by the design requirements. Based on the design requirements, a prototype is described which is tested and discussed afterward. Finally, the third part of this thesis will discuss the results of the first, and second part in the broad context of this study.

The dashed lines in Figure 1.5 refer to the relation between the first part and the second part of this thesis. During the pilot study, it is determined which type of tag defines the dimensions of the first design prototype. During the work on in-vivo approvals, information about CE-marking[1] of instruments is acquired that defines design requirements for the prototype of the attachment.

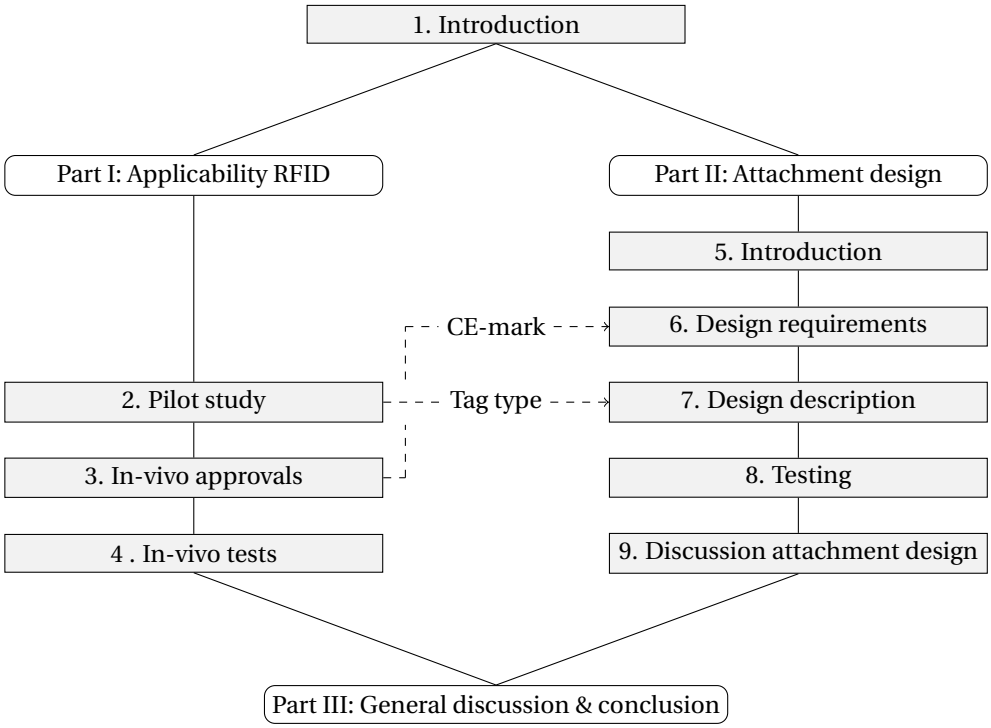

Figure 1.5: Outline thesis.

[1] According to [27], "CE Marking on a product is a manufacturer's declaration that the product complies with the essential requirements of the relevant European health, safety and environmental protection legislation, in practice by many of the so-called Product Directives".

I

Applicability RFID

2

Pilot study

A pilot study is executed in a near-surgical setting to evaluate the applicability of an RFID-setup to identify instruments, which is intended to be used during in-vivo tests. This pilot study is related to eventual in-vivo tests in such a way that the results are incorporated into the process of realizing in-vivo testing and to determine whether the RFID-setup performs sufficiently. During this pilot study, a total of 10 TEP-procedures were mimicked at an OR at location Voorburg of RdGG, where all surgical equipment and devices necessary for a TEP-procedure were present. The procedures were mimicked using several instructional online videos that display the consecutive steps of a TEP-procedure. For the pilot study, a selection of the complete set of surgical instruments for a TEP-procedure was equipped with RFID-tags by Van Straten Medical BV, the Netherlands. The RFID-tags are attached to the instruments by means of two stainless steel counterparts which fit around the instrument. The counterparts are either welded together or fixed by a screw. The tags are located on top of the attachment and encapsulated by epoxy to protect the tag against impacts and the extreme conditions during the sterilization process. Figure 2.1 shows an example of the tagged instruments.

Figure 2.1: Example of an instrument, as tagged by Van Straten Medical BV. The tag is encapsulated in an epoxy to protect it against impacts and extreme conditions during the sterilization process.

2.1. Method

A distinction can be made between the identification of instruments that are considered to be currently 'in-use' by the surgeon, or 'idle'. Basically, when identifying idle instruments, the data of instrument usage is based on instruments that are *not* being used. The opposite applies to the identification of 'in-use' instruments. One of the two methods has to be chosen for this study. Instruments in an 'idle' stage can be identified when located on the operating table [28], or mayo stand. However, observations during the attendance at several surgeries prior to this study learned that instruments are not naturally returned to the instrument table or mayo stand when not being used any longer. Figure 2.2 shows an example where an instrument that is not being used any longer is located on a random cabinet in the OR.

Figure 2.2: Instruments that are not used any longer are not naturally returned to the instrument table.

Instruments that are not returned to the instrument table or mayo stand will not be identified and thus not registered as 'idle', resulting in false negative identifications. Instrument identification of 'in-use' instruments does not depend on the location of idle instruments and is therefore considered as less susceptible to false identifications. Hence, the identification of 'in-use' instruments is applied in this study.

This section describes the RFID-setup that is used to identify the tags that are attached to the instruments, followed by the equipment that is used, the test setup, the test procedure, and the method of transforming the acquired data for further analysis.

2.1.1. RFID-setup

A schematic overview of the RFID-setup as used in this pilot study is presented in Figure 2.3. The reader, which is powered through a power outlet, communicates with the computer using Ethernet. The antenna is connected to the reader by means of a coax cable, and can detect tags withing its reading range. The software on the computer presents the data from the reader to the user in a readable form, and it provides configuration options for the readers' settings.

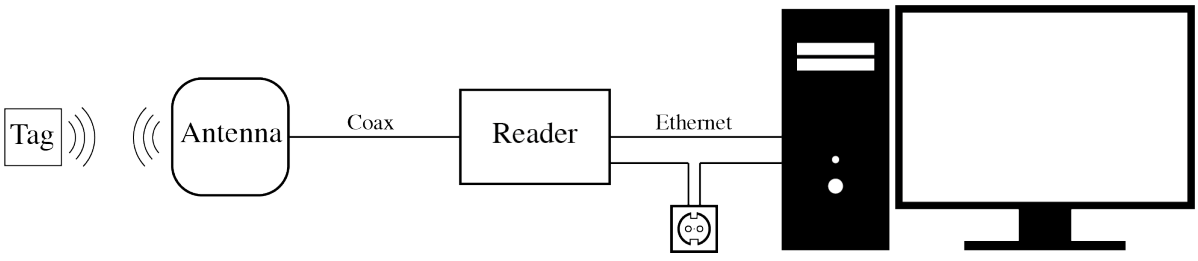

Figure 2.3: Schematic overview of the RFID-setup.

Reader

The reader "Ha-VIS RF-R500-c" (HARTING Deutschland GmbH & Co. KG, Minden, Germany) is used upon availability by the Technische Universiteit Delft (TUD). The reader operates at 2W.

Antenna

Two antennas were made available by the Technische Universiteit Delft (TUD) during this study. The first antenna is the Ha-VIS RF-ANT-MR20-EU (HARTING Deutschland GmbH & Co. KG, Minden, Germany), which operates at 0.5W ERP. The second antenna is the Ha-VIS RF-ANT-WR30-EU (HARTING Deutschland GmbH & Co. KG, Minden, Germany), which operates at 2W ERP. Previous research evaluated the performance of the two antennas [29]. The first antenna was concluded to perform insufficiently for a surgical setting, due to its smaller radiated power. The second antenna, however, showed great potential. Thus, the antenna used for this study is the Ha-VIS RF-ANT-WR30-EU (HARTING Deutschland GmbH & Co. KG, Minden, Germany). The antenna operates at 2W in the frequency range of 865-870 Mhz, which is UHF.

Tags

The tags that are used during this study are the Xerafy Dot XXS (Xerafy, Singapore, Singapore), Xerafy Dot XS (Xerafy, Singapore, Singapore), HID Brick 75 (HID Global, Austin, USA), and HID Brick 60 (HID Global, Austin, USA). The specifications of the tags are listed in Table 2.1.

Table 2.1: Tags, with specifications, that are used during this pilot study.

	Xerafy Dot XXS	**Xerafy Dot XS**	**HID Brick 75**	**HID Brick 60**
Size [mm]	⌀ 4.08 x 2.58	⌀ 6 x 2.5	5 x 5 x 3	10 x 2.5 x 2.5
Mounting method	Adhesive,embedded	Adhesive	Adhesive/enclosure	
Autoclavable	Yes			
Affixes to	Metal			
Reading distance [m]	0.5	1.5	1.0	1.0
Operating frequency	866-868 MHz (UHF)		869 MHz (UHF)	
Type	Passive			

The choice for the types of tags that are used during this study is based on the availability of the tags to Van Straten Medical BV. Also, tags with different dimensions are applied, considered that there is a trade-off in performance and discomfort experienced by the surgeon and OR-personnel. All of the aforementioned tags are passive tags, meaning that they do not require an internal battery to power their circuitry. Active tags are considered to be impractical to attach to surgical instruments, due to dimensions and the presence of an additional power source.

Software

Harting RFID-config software (HARTING Deutschland GmbH & Co. KG, Minden, Germany) is used to configure and control the reader. The software presents a list of all detected tags to the user, showing the tag-id, date, and time of the detection. Also, as soon as the measurement is stopped by the user, the software generates a text file containing a log file of all detected tags within the timeframe of the measurement. From now on, the Harting RFID-config software (HARTING Deutschland GmbH & Co. KG, Minden, Germany) is referred to as RFID-software.

2.1.2. Instruments and surgical steps

The selection of the instruments that is used during this pilot study contains all the required instruments needed to mimic all the steps of a TEP-procedure. The list of instruments used in this pilot study is presented in Table 2.2. The choice of the type of tag that is attached to the instruments is based on the availability of the tags. Also, instruments of the same type (e.g. Trocar 5mm #1 and Trocar 5mm #2) are not equipped with the same type of tag, in order to evaluate the varying performance between different types of tags.

The TEP-procedure is divided into ten surgical steps. The surgical steps are inspired by surgery reports [26] and discussed with Dr. Maarten van der Elst. Table 2.3 shows the ten surgical steps, combined with the instruments from Table 2.2 that are used during the steps. The function of the tag that is attached to instrument number 12, the cup, is explained later.

Table 2.2: List of instruments that are equipped with tags.

Instrument no.	**Instrument name**	**Tag-type**
1	Scalpel handle	HID Brick 75
2	Langenbeck retractor	HID Brick 60
3	Trocar 11mm	HID Brick 60
4	Endoscope	Xerafy XS
5	Trocar 5mm #1	Xerafy Dot XXS
6	Laparoscopic handle #1	HID Brick 60 m
7	Trocar 5mm #2	Xerafy XS
8	Laparoscopic handle #2	Xerafy Dot XXS
9	Electrosurgery cable	Xerafy Dot XXS
10	Tweezer	Xerafy Dot XXS
11	Needle forceps	HID Brick 75
12	Cup	HID Brick 75

Table 2.3: List of consecutive steps in a TEP-procedure vertically, and horizontally the instrument numbers, as presented in Table 2.2, in use during the steps.

	1	2	3	4	5	6	7	8	9	10	11	12
1. Introduction first trocar	X	X	X	X								
2. Introduction second trocar	X		X	X	X							
3. Introduction third trocar	X		X	X	X		X					
4. Identification of crucial parts* and hernial sac			X	X	X	X	X	X	X			
5. Identify hernia type (direct/indirect)			X	X	X	X	X	X	X			
6. Reduction of the inguinal hernia			X	X	X	X	X	X	X			
7. Introduction of preperitoneal mesh			X	X	X	X	X	X	X			
8. Placement and fixation of preperitoneal mesh			X	X	X	X	X	X	X			
9. Wounds closure										X	X	

*= epigastric veins, os pubis, Cooper's ligament, funiculus/rotundum

2.1.3. Test setup

Tasks

The pilot study was performed with an additional researcher, as the tests included more tasks than one person could perform. One of the researchers fulfilled the role of the surgeon, while to other researcher acquired the data and provided the necessary surgical instruments to the surgeon.

Setup

Figure 2.4 shows the location of the instrument table, the researchers, and the RFID-equipment during the pilot study. Both the RFID-laptop and the Matlab-laptop are used for data acquisition. The antenna is mounted to an infusion pole by means of a ball joint. The infusion pole enables free movement of the antenna through the OR, and the ball joint allows for an adjustment of the inclination and height of the antenna. The antenna is located at the side of the operating table and facing toward the surgical area. The surgical area is defined as the area in which the surgical actions are performed. In the case of a TEP, the surgical area is considered to be an imaginary box with dimensions 0.5mx0.5mx0.5m (lxwxh). These dimensions are based on the maximum length of laparoscopic tools. The antenna is located as close as possible to the surgical area, while not inducing any discomfort to the researchers. A Video-laptop is located next to the researcher that acts as a surgeon to display the explanatory TEP-procedure videos.

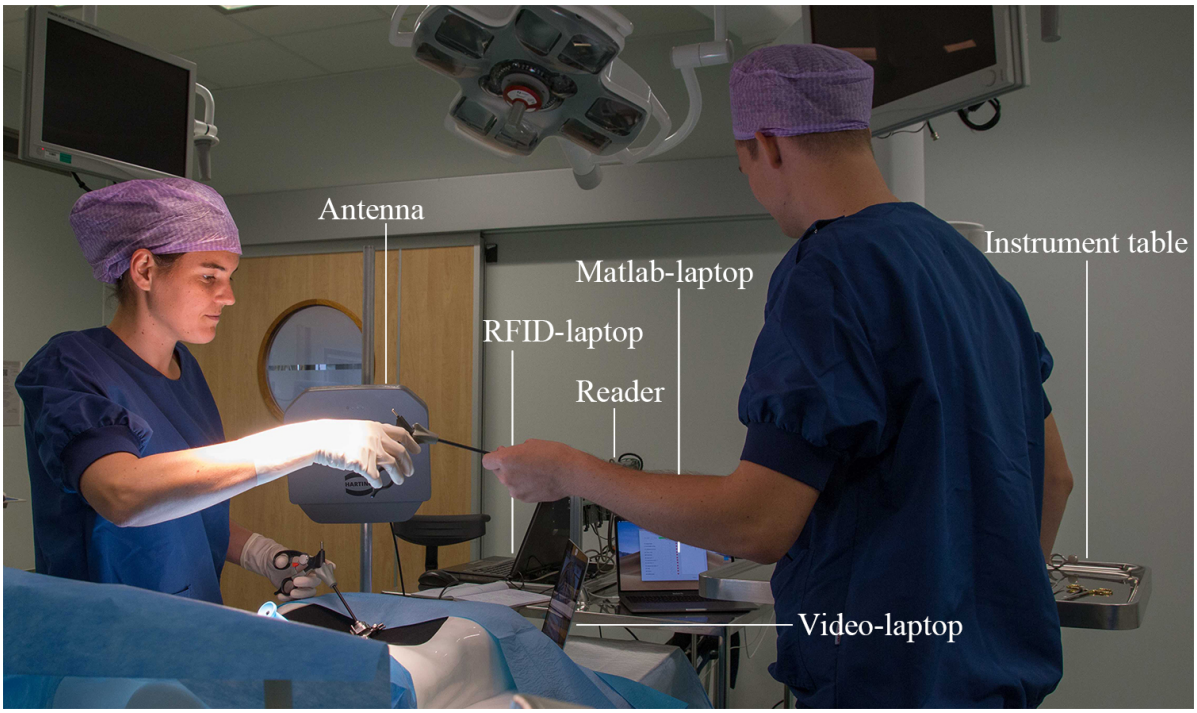

Figure 2.4: Overview of the location of the instrument table, researchers and the RFID-equipment during the pilot study.

Validity

The RFID-laptop, to which the reader is connected, is facing away from the researchers, to prevent the researchers from seeing the detection results and therefore unintentionally induce deviations in their actions to improve the outcomes. During this pilot study, all equipment that could potentially interfere with the RF-waves was turned on. This concerned the following equipment: Anaesthesia workstation, patient monitoring system, syringe pump, and the electrosurgery hardware. The researcher that fulfilled the role of the surgeon was wearing surgical gloves to prevent potential detuning of the RF-waves through conduction via the body. Diversity in the testing procedure is introduced because a total of 7 different online videos are used to mimic TEP-procedures. The separate surgical steps within the videos varied in duration.

Data acquisition

During the tests, each detection of a tag by the antenna was registered within the RFID-software that ran on a laptop (Dell Latitude D630, Intel Core 2 Duo Mobile T7500). Besides the RFID-software, an additional Matlab-script, written in the Matlab software (Mathworks Inc., Massachusetts, USA), ran on a separate laptop (MacBook Pro, 2Ghz Intel Core i5) to manually annotate the actual times of inserting and withdrawing of instruments into, and out of the surgical area. The data of the actual usage time of the instruments are necessary for the validation process of the data of the detection that originates from the RFID-software. The Matlab-script saves the data into a Matlab structure for further data analysis. Figure 2.5 presents a window of the Matlab-script, showing an example of the information as provided to the user. The window shows a list of the instruments that are used, with the ability to register the insertion- and withdrawal time of the instruments. The green and red lights indicate that an instrument is either located inside (green) or outside (red) of the surgical area. The table with times, and the remaining buttons function for archiving of the data.

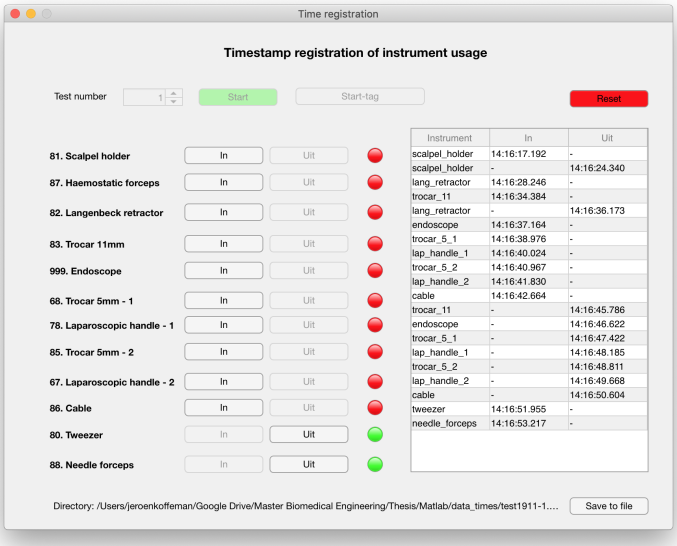

Figure 2.5: Example of the window from the Matlab-script as presented to the user. A list of all instruments is visible, with the option to register the insertion- and withdrawal time of the instruments.

2.1.4. Test procedure

The RFID-setup was set as described in Section 2.1.1, and the complete testing equipment was set as described in Section 2.1.3. Both the RFID-software and the Matlab-script are launched, but not yet started. The anaesthesia workstation, patient monitoring system, syringe pump, and electrosurgery hardware are turned on. From now on, the preparation is finished, and a single test can be executed: (1) The RFID-software is started, which activates the antenna. Also, (2) the Matlab-script is started, which is followed by (3) holding instrument 12 (Table 2.2), the cup, in front of the antenna. The tag that is attached to instrument 12 is considered a 'start-tag'. As soon as this tag is detected by the antenna, (4) the button 'Start-tag' on the Matlab-script is clicked (see Figure 2.5), which registers the date and time of the detection of the 'start-tag'. This step is necessary due to an incorrect registration of date and time by the reader. During data analysis, the manual date and time registration of the start-tag is used to compensate for the error in date and time as registered by the reader. Next, (5) an instructional TEP-procedure video is started on the video-laptop, after which (6) the steps of the video are re-enacted by the researchers. Whilst the instructional video is running, one researcher acts as a surgeon, and the other 'assistant' researcher provides the 'surgeon' with the necessary instruments (see Figure 2.4). Simultaneously, the 'assistant' researcher manually registers the time of insertion and withdrawing of the instrument into and from the surgical area using the Matlab-script. After completion of the mimicked TEP-procedure, (7) the results of the RFID-software and the Matlab-script are saved into log files and reset. A new test can now start, starting at step (1).

2.1.5. Data transformation

Table 2.4 shows five explanatory entries of data as extracted from the RFID-software, which is referred to as 'antenna data' from now on. Each row provides the n^{th} number of detection (No) since the first detection, followed by an identifier (TrType) that is used by the reader to decode the signal. Then, the Tag-ID is displayed as 'UID', followed by the date, time, and the antenna number (AntNo). Since only a single antenna is used during this pilot study, the antenna number will always be equal to 1. Note that the reader does not register the date and time correctly, and thus, a correction is required, using the registration of the 'start-tag'. For example, the detection of the 'start-tag', as presented in Table 2.4, occurred at 18:25:10.180. However, the 'start-tag' is manually registered at 13:25:10.180, and thus, a correction of 5 hours must be applied to the antenna data. The Tag-ID's are listed in Table 2.5.

Table 2.4: Explanatory entries of data as extracted from the antenna, where the first detection is the start-tag.

No	TrType	UID	Date	Time	AntNo
1	0x84	E2003098010702352160 35F7 (start-tag)	2077-22-28	18:25:10.180	1
...	...	...	...	...	...
100	0x84	E2003098971301082310295C	2077-22-28	18:30:10.180	1
101	0x84	E2009A5010030AF000001919	2077-22-28	18:30:10.349	1

Table 2.5: List of the used instruments, with the ID's of the applied tags.

Instrument no.	Instrument name	Tag-ID
1	Scalpel handle	E2003098010401031110A954
2	Langenbeck retractor	E20030989713019224801A2B
3	Trocar 11mm	E2003098971301082310295C
4	Endoscope	E2009A5010030AF000001919
5	Trocar 5mm #1	E2009A7030031AF000003517
6	Laparoscopic handle #1	E20030989713020420 10461F
7	Trocar 5mm #2	E2009A7050010AF000000083
8	Laparoscopic handle #2	E2009A7030031AF000003601
9	Electrosurgery cable	E2009A7050010AF000000025
10	Tweezer	E2003098010702040460E7EC
11	Needle forceps	E2009A7050010AF000000023
12	Cup	E2003098010702352160 35F7 (start-tag)

For the purpose of phase recognition, the data, as extracted from the antenna is transformed into a time-based dataset containing an entry for each second since the start of the surgery. An example of a single entry is as follows: As presented in Table 2.4, the tags with their UID that refer to instrument numbers 3 and 4 (Table 2.5) are detected within one second. This occurred at 300 seconds (5 minutes) since the detection of the start-tag (see Table 2.4). This data is then transformed into an entry as presented in Table 2.6, where the columns with the numbers 1 to 11 refer to the instrument numbers as defined in Table 2.5, and present the instrument usage as binary data, where 1=detected, and 0=not detected. This entry is from now on referred to as antenna-entry. The Surgery ID is generated based on the order in which the different tests took place during the pilot study. Note that for this data transformation, the correction of date and time is not necessary since the dates and times are converted to a duration list.

Table 2.6: antenna-entry of the time-based logfile after transformation of the data. The columns with numbers 1 to 11 refer to the instrument numbers.

Surgery ID	Surgery Duration [s]	1	2	3	4	5	6	7	8	9	10	11
3	300	0	0	1	1	0	0	0	0	0	0	0

The manually annotated data is also converted to a time-based log which matches the structure of Table 2.6. This is referred to as manual-entry from now on.

2.2. Surgical phase recognition

To evaluate the performance of the RFID-setup, a surgical phase recognition model is constructed. In general, such a model is generated using a training dataset, with known output, after which testing data can be validated. Essentially, the testing dataset is equally structured as the training dataset, only that the output is yet unknown. This output is estimated using the surgical phase recognition model. From a selection of machine learning models that are applicable to surgical phase recognition, the Random Forest model shows the best performance in laparoscopic hysterectomy procedures [2]. Laparoscopic hysterectomy procedures are considered similar to TEP-procedures, based on the types of instruments that are used. Thus, a Random Forest model is applied to evaluate the performance of the RFID-setup that is used in this pilot study. The Random Forest model as presented in this thesis is written in Python (Python Software Foundation, Wilmington, USA), using a selection of mathematical modules and the RandomForestClassifier module provided by Scikit-learn [30].

2.2.1. Phases

As mentioned in the introduction, the aim of a surgical phase recognition models is to reconstruct the phases, based on low-level sensor information. In this study, the low-level sensor information is acquired using the RFID-setup. Thus, in order to construct a Random Forest model, the surgical steps of a TEP-procedure as defined in Table 2.3 are empirically transformed into four consecutive phases:

Phase 1: Step 1
Phase 2: Steps 2,3
Phase 3: Steps 4,5,6,7,8
Phase 4: Step 9

Note that Phase 3 consists of all the laparoscopic steps, because no change in instrument usage occurs in those steps.

Table 2.7 highlights how the phases are characterized by the insertion or withdrawal of certain instruments into or from the surgical area. For example, phase 3 starts when both the laparoscopic handles are inserted into the surgical area. Phase 3 stops when all the laparoscopic instruments (instrument numbers 3,4,5,6,7,8,9) are withdrawn from the surgical area. Note that instrument number 2, the 'Langenbeck retractor', is not included in Table 2.7 since its insertion or withdrawal does not contribute to the characterization of a single phase.

Table 2.7: The four phases of a TEP-procedure, that are characterized by the insertion or withdrawal of certain instruments.

	Phase 1		**Phase 2**		**Phase 3**		**Phase 4**	
	Start	**Stop**	**Start**	**Stop**	**Start**	**Stop**	**Start**	**Stop**
1. Scalpel handle	in							
3. Trocar 11mm		in	in			out		
4. Endoscope						out		
5. Trocar 5mm #1						out		
6. Laparoscopic handle #1				in	in	out		
7. Trocar 5mm #2						out		
8. Laparoscopic handle #2				in	in	out		
9. Electrosurgery cable						out		
10. Tweezer							in	out
11. Needle forceps							in	out

2.2.2. Random Forest

A Random Forest model is a machine learning method for classification or regression, that is constructed using a collection of decision trees [31]. A decision tree maps all possible outcomes of a target value, based on decision rules that are generated from data features (Appendix C) [32]. Figure 2.6 illustrates a simplified representation of a decision tree, where the phase is determined based on the usage information of a tweezer during surgery. The rectangles represent conditions, which are split into branches. Branches that do not split anymore are considered decisions and are represented by the rounded rectangles. Decision trees can be modeled as regression- or classification trees, where regression trees result in a continuous value (e.g. 1.0 or 1.1) and classification trees in a categorical value (e.g. 1 or 2). The final decision of a random forest model is either the mean value (regression) or mode (classification) of all the decision trees outcomes [2]. For the application of phase-recognition in TEP-procedures, classification trees are considered most suitable. Classification trees assign the outputs of a Random Forest model to a class, which, in case of the TEP-procedure are the possible surgical phases (Table 2.7). Regression trees are shown to be relevant when predicting for instance end times of surgeries [2].

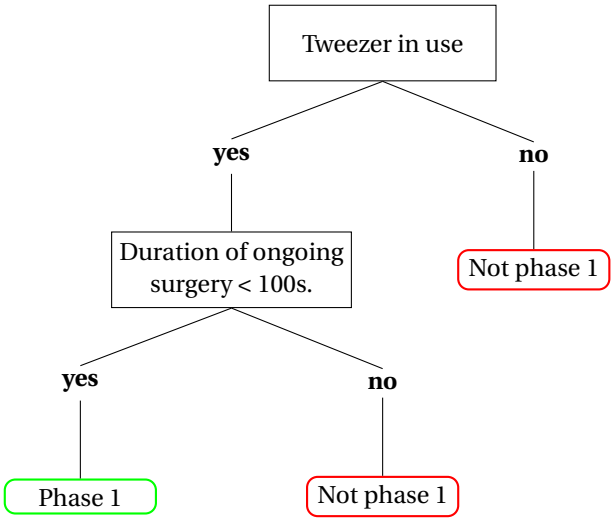

Figure 2.6: Simplified decision tree example; rectangles represent conditions, which are split into branches. Branches that do not split anymore are decisions, which are represented by rounded rectangles.

The construction of the Random Forest model as used in this study is visualized in Figure 2.7. During this pilot study, 10 logfiles of manually annotated data and 10 logfiles of antenna data were extracted from the 10 mimicked TEP-procedures. The manually annotated data is transformed, as described in Section 2.1.5. A total of 10 logfiles is considered as an insufficient amount of data to construct an accurate Random Forest model. Also, the 10 original logfiles of manually annotated data are intended to be used as validation of the antenna data. Therefore, the transformed data is processed with a Randomizer to simulate 30 separate logfiles containing data that is based on the original manually annotated logfiles. Based on the phases as defined in Table 2.7, the phase for each entry of the transformed manually annotated data is defined. The phase is then added as a column to the manual-entry. A similar process is applied in Feature Engineering. Data features (e.g. number of instruments currently in use) are derived from the instrument usage since a single entry from the simulated log files does not include sufficient information to train a Random Forest model. Please refer to Appendix C for an in-depth elaboration on the feature engineering process. The phases, the simulated 30 log files, and the features are combined into a training set, which is then used to construct the final Random Forest model.

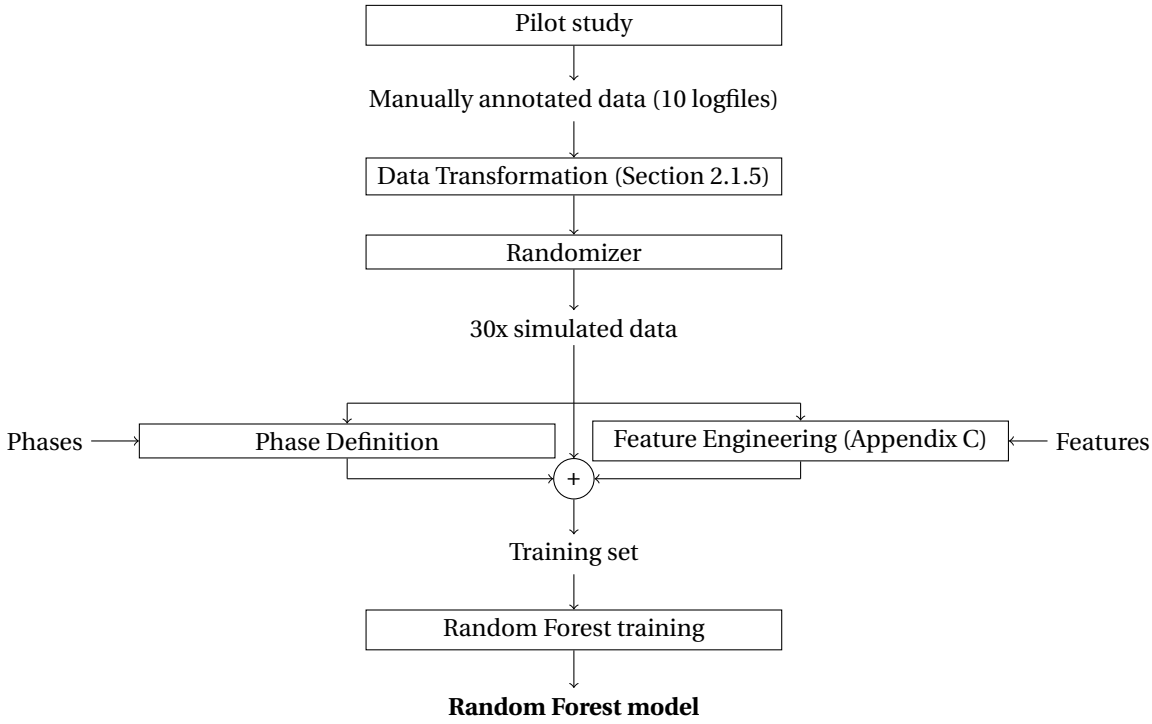

Figure 2.7: Overview of the construction of a Random Forest model; the Manually annotated data from the Pilot study is transformed and 30 simulated logfiles are generated. A training set results after Phase Definition, and Feature Engineering, which is then used to train a Random Forest model.

Table 2.8 presents an example entry of the training set, which is an expansion of the manual-entry. Note the addition of the phase column and the feature columns, which starts with the first feature 'No. instruments in use'. Again, the columns with numbers 1 to 11 refer to the instrument numbers, where the instrument usage is presented as binary. The Random Forest model uses a collection of one hundred decision trees, based on [2].

Table 2.8: Example of training dataset after data transformation, phase definition and feature engineering.

Surgery ID	**Phase**	**Surgery Duration [s]**	**1**	**...**	**11**	**No. instruments in use**	**...**	**n^{th} Feature**
3	2	300	0	...	0	2	...	...

Given the Random Forest model, as constructed according to Figure 2.7, the antenna data can be validated using this model to estimate the phase for each entry of the log file. The validation process is visualized in Figure 2.8. The process chart shows both data from the manual log files and the antenna log files being transformed. After transformation, the data from the manual log files is directly processed through Phase Definition, resulting in the actual phases. On the right side, after transformation, the data from the antenna log files is processed through Feature Engineering. Note that the phases are not defined for the antenna log files since the antenna log files are considered to include missing data points and errors and therefore, the phases are going to be estimated by the Random Forest model. The actual phases from the manual log files and the predicted phases from the antenna log files are then compared in the Validation process, resulting in an accuracy. This accuracy represents the ratio to which extent the predicted phases match the actual phases.

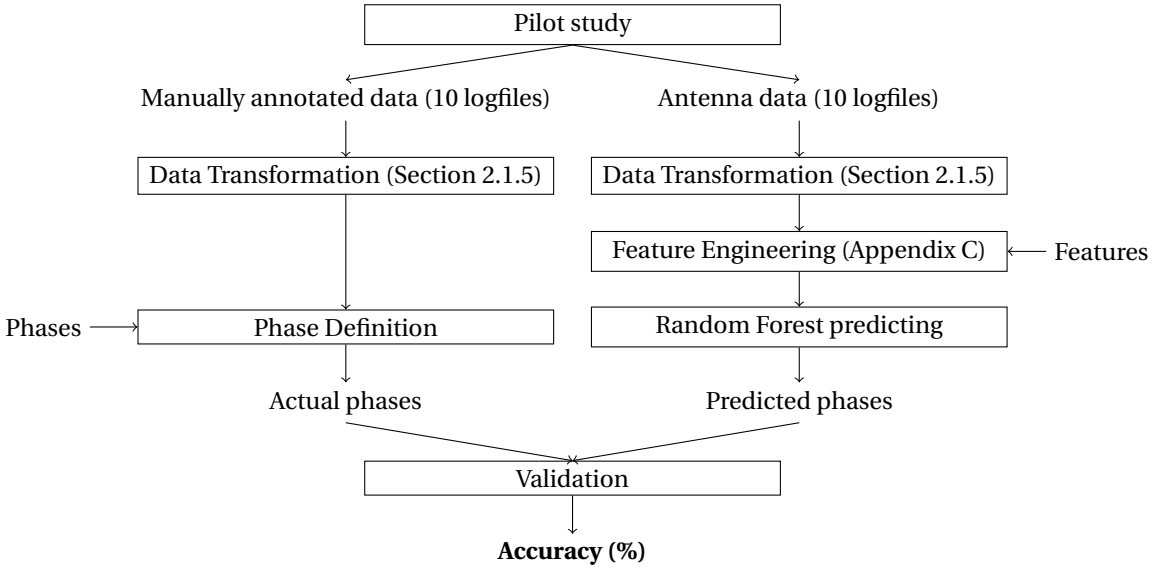

Figure 2.8: Overview of the validation process of the Antenna data. Both the Manually annotated data and Antenna data are transformed. The phases of the Manually annotated data are defined, resulting in the actual phases. The Features of the Antenna data are engineered, after which the phases of the Antenna data are predicted using the Random Forest model. The actual phases are compared with the predicted phases, resulting in an accuracy.

2.3. Results

The mimicked TEP-procedures showed an average surgery time of 13 minutes and 52 seconds. The results are divided into the raw data, the Random Forest results, and the acceptance results.

2.3.1. Raw Data

Figure 2.9 shows the raw data of a single test, after time- and date correction. For each instrument that was used during the test, a subplot is visible, and the x-axis displays the time of the surgery. A red rectangle represents the manually annotated data, and the blue dots refer to the moments of detection by the antenna. Please refer to Appendix D for the plots of the remaining 9 tests. Besides the 'Langenbeck retractor', the raw data indicates that the instruments are, with a few exceptions excluded, not detected whilst being located at the instrument table. Thus, very few false positives occurred.

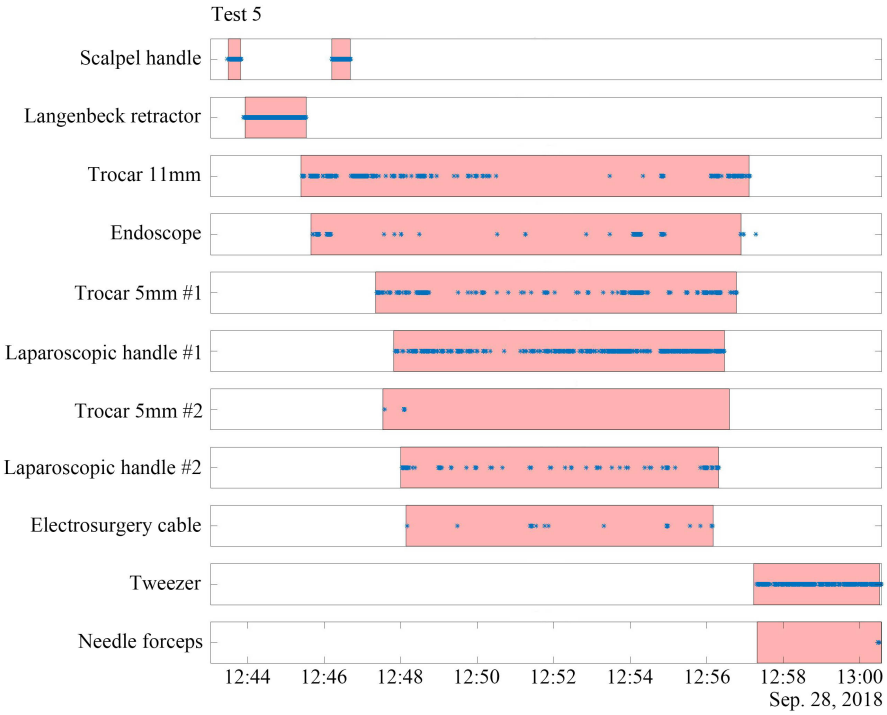

Figure 2.9: Raw data of a single test during the pilot study after time- and date corrections are applied. A subplot is presented for each instrument showing the actual usage in a red rectangle, and the detection of the tags that are applied to the instruments are presented as blue dots.

Figure 2.10 shows the same test results, but with an additional overlay of the defined phases according to Table 2.7. Phase 1 starts at the insertion of the 'Scalpel handle' into the surgical area. Phase 2 starts when 'Trocar 11mm' is inserted. Phase 3 starts when both laparoscopic handles are inserted. Lastly, Phase 4 starts when all the laparoscopic instruments are withdrawn, and both the 'Needle forceps' and 'Tweezer' are inserted.

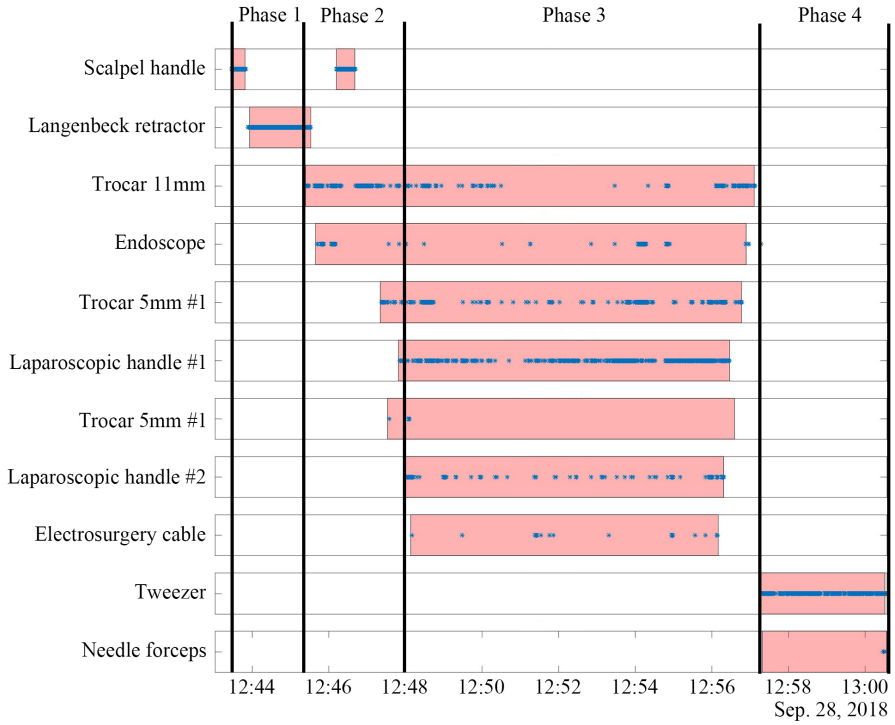

Figure 2.10: An additional overlay over the raw data from Figure 2.9 that shows the defined phases according to Table 2.7. Phase 1 starts at the insertion of the 'Scalpel handle' into the surgical area. Phase 2 starts when 'Trocar 11mm' is inserted. Phase 3 starts when both laparoscopic handles are inserted. Phase 4 starts when all the laparoscopic instruments are withdrawn, and both the Needle forceps and Tweezer are inserted.

2.3.2. Random Forest Results

The Random Forest model achieved an accuracy of 92.7%, with a computational time of 0.27 seconds for the prediction, for a total of 8810 entries. This means that the phase was correctly estimated for 92.7% of the entries of the antenna log files. The results are visualized in Figure 2.11, which shows the confusion matrix. A confusion matrix depicts the accuracy of the Random Forest results. The vertical axis represents the actual phase, while the horizontal axis refers to the phases that are predicted by the Random Forest model. The numbers inside the squares refer to the number of entries of which the phases are predicted. For example, for 33 entries, the Random Forest model predicted phase 2, while it should have been phase 3. The greatest error is shown while predicting phases 1 and 2. For 390 entries, the Random Forest model predicted phase 1, while it should actually be phase 2.

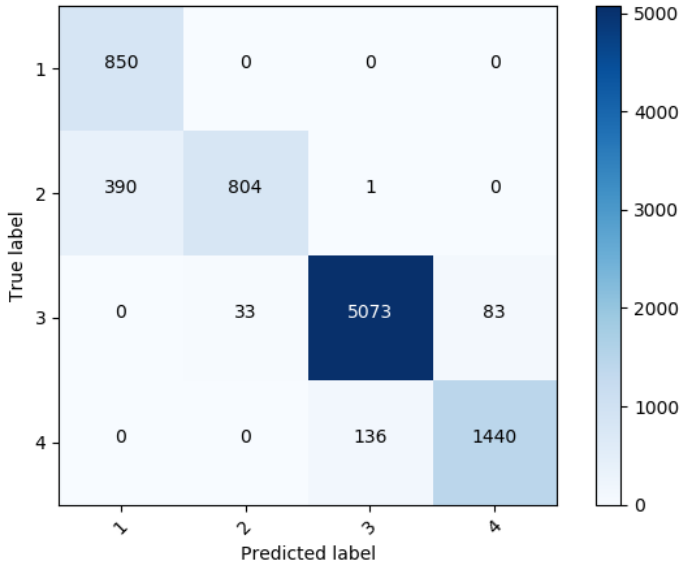

Figure 2.11: Confusion matrix; the vertical axis represents the actual phase, while the horizontal axis refers to the phases that are predicted by the Random Forest model. The numbers inside the squares refer to the number of entries from which the phases are predicted.

2.3.3. Acceptation

The tags that were attached to the surgical instruments did not induce discomfort of any kind to both researchers. Also, the location of the antenna did not interfere with the movements of the researchers. The reader is connected to the antenna using a coax cable with a length of 3 meters, and thus, it can be located at a distance where it does not interfere with any personnel.

2.4. Discussion Pilot study

In this pilot study, the applicability of an RFID-setup is evaluated in a near-surgical setting. A total of 10 TEP-procedures are mimicked using a selection of the instrument set that is used during a TEP-procedure. The instruments that are equipped with tags can be detected by the RFID antenna. The RFID-setup that is used during the pilot study is evaluated on acceptance, and performance using a Random Forest model to estimate the surgical phase for each entry in the antenna data.

The raw data indicates that the instrument 'Trocar 5mm #2' is poorly detected throughout the tests. According to Table 2.2, 'Trocar 5mm #2' is equipped with a Xerafy Dot XS tag. However, the same type (shape, dimensions, material) of instrument 'Trocar 5mm #1' is equipped with a Xerafy Dot XXS tag. One would expect that the smaller tag (Dot XXS), due to its smaller effective area of absorbing RF-waves, would perform worse. However, the raw data indicates the opposite, where 'Trocar 5mm #1' with a Xerafy Dot XXS tag performs significantly better in most cases. Another explanation for the poor detection of 'Trocar 5mm #2' regards the location when the instrument is used within the surgical area. However, Figure 2.12 indicates otherwise. Figure 2.12a shows the location of 'Trocar 5mm #2', while Figure 2.12b shows the location of the endoscope (note: picture was taken from the opposite side of the operating table). Both 'Trocar 5mm #2' and the endoscope are equipped with a Xerafy XS tag. Despite the fact that the endoscope is also not detected very often, it still performs better than the 'Trocar 5mm #2', while being located at a greater distance from the antenna.

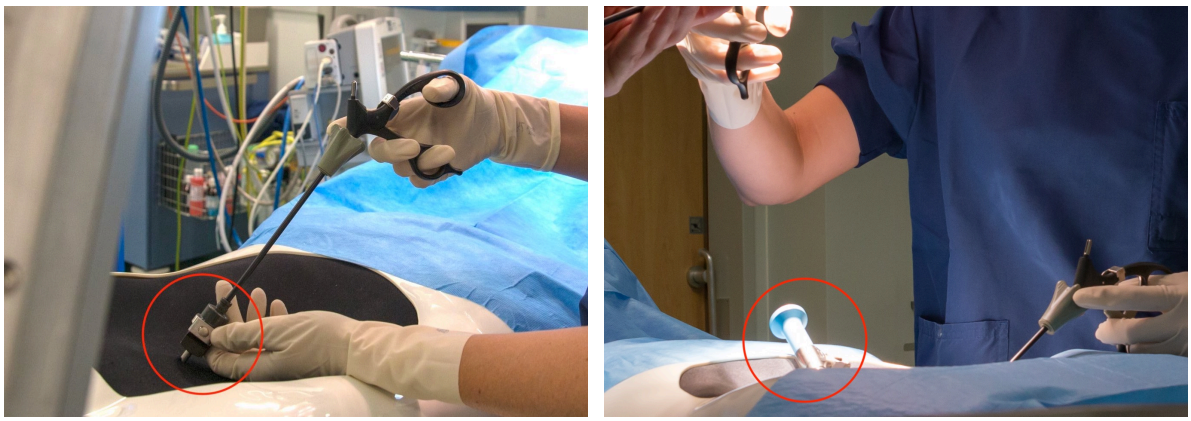

(a) Location of 'Trocar 5mm #2' (encircled) when located within the surgical area.

(b) Location of the 'Endoscope' (encircled) when located within the surgical area.

Figure 2.12: Location of 'Trocar 5mm #2' and the 'Endoscope' when used within the surgical area.

The detection performance is assumed to depend on a selection of factors: total area of the instrument to which a tag is attached, which defines the area that can absorb RF-waves; the movement of the instrument during usage, which increases the chance of detection; the deflection of RF-waves by means of surrounding instruments; and whether the tag is facing towards the antenna or away from the antenna. In case of the 'Trocar 5mm #2', the factors that affect the detection are not considered to be directly applicable, and thus, the tag that is equipped to the 'Trocar 5mm #2' might be defective.

An accuracy of 92.7% is achieved using the Random Forest model. One can argue that the model is not yet optimized on accuracy and process time. However, within the scope of this research, an accuracy of 92.7% is considered sufficient to show the potential of the RFID-setup. Also, the model is not (yet) used as a real-time estimator, and therefore, the computational time is not relevant. The confusionmatrix from Figure 2.11 showed the greatest error while predicting phases 1 and 2. For 390 entries, the Random Forest model predicted phase 1, while it should actually be phase 2. This error is presumably induced by an assumption that is made when generating the Random Forest model, where the instrument 'Scalpel handle' is used only once, at the beginning of phase 1. However, the raw data (Appendix D) shows an additional usage of the Scalpel handle during phase 2, which likely causes misinformation to the model.

The performance of the RFID-setup is achieved while the antenna was positioned at a location that was considered to be the best option by the researchers, regarding the detection performance and discomfort. However, the researchers are likely to be biased and thus, the surgeon might not be as satisfied with the position of the antenna as the researchers were. A less optimal position of the antenna is therefore expected during an in-vivo test. Nevertheless, the surgical actions were not interfered with in any way by the antenna, and the tags that are attached to the instruments did not induce any discomfort.

A request for an in-vivo test will not be accepted by the hospital until a selection of strict regulations is complied with. The literature does not show a one-sided conclusion on whether electromagnetic interference will occur between the antenna and surrounding medical equipment. During this pilot study, the surrounding medical equipment was turned on, but not activated. Although no interference was noticed, it is yet to be evaluated at a surgical setting in which an in-vivo test will take place while the equipment is active. Also, the RF-waves that are emitted by the antenna must be tested on field strength, since the surgical equipment is only guaranteed to function properly up to certain limits of radiation. Finally, the criteria of whether an in-vivo test with the RFID-setup that is used during this pilot study will be bound to informed consent is yet to be determined.

In conclusion, the RFID-setup has shown the potential to provide relevant data for a phase recognition model to estimate the surgical workflow during surgery. Also, the RFID-setup is not expected to induce any discomfort to the OR-personnel. However, several regulations are yet to be complied with in order for an in-vivo test to be accepted.

3

In-vivo approvals

This chapter describes the approvals that are required to perform an in-vivo test. Section 3.1 presents the procedure that is required for an in-vivo study to be accepted, of which a selection of steps was already finished prior to this study. Within the timeframe of this study, a selection of approvals was obtained regarding patients' consents (Section 3.3), the applicability of the RFID-equipment into a surgical setting (Section 3.4), and the sterilizability of the instruments that are equipped with tags (Section 3.5). For this chapter, the research that is executed during this study is referred to as 'RFID-research'.

3.1. Overview

This section provides a brief overview of the approval process that is required for in-vivo testing. The overview is schematically presented in Figure 3.1. The process starts with a protocol of the study that is presented to the Medische Ethische Toetsingscommissie (METC). The METC is an independent commission that is competent to declare whether research is within scope of the 'Wet medisch-wetenschappelijk onderzoek met mensen (WMO)'. The WMO is further elaborated on in Section 3.2. Note that WMO obligated research is subject to review by the METC. Not-wmo obligated research, on the contrary, must comply with the procedures of the concerned institution where the research takes place. After the declaration of 'not-WMO' obligated, the protocol and the WMO-declaration are presented to the board of directors of the concerning hospital, which in this case is RdGG. The accepted protocol is communicated with the TU Delft, after which the instruments are sent to Van Straten Medical BV to get equipped with tags. Both the RFID-equipment and the tagged instruments are presented to a clinical physicist of RdGG to be judged on whether it can be applied into a surgical setting. The tagged instruments are also presented to Combi-ster, which is the Central sterile services department (CSSD) of RdGG, to evaluate the sterilizability. The protocol and equipment are discussed with the surgeon, and after a 'Green light' of both Combi-ster and the surgeon, the final protocol is composed by the TU Delft.

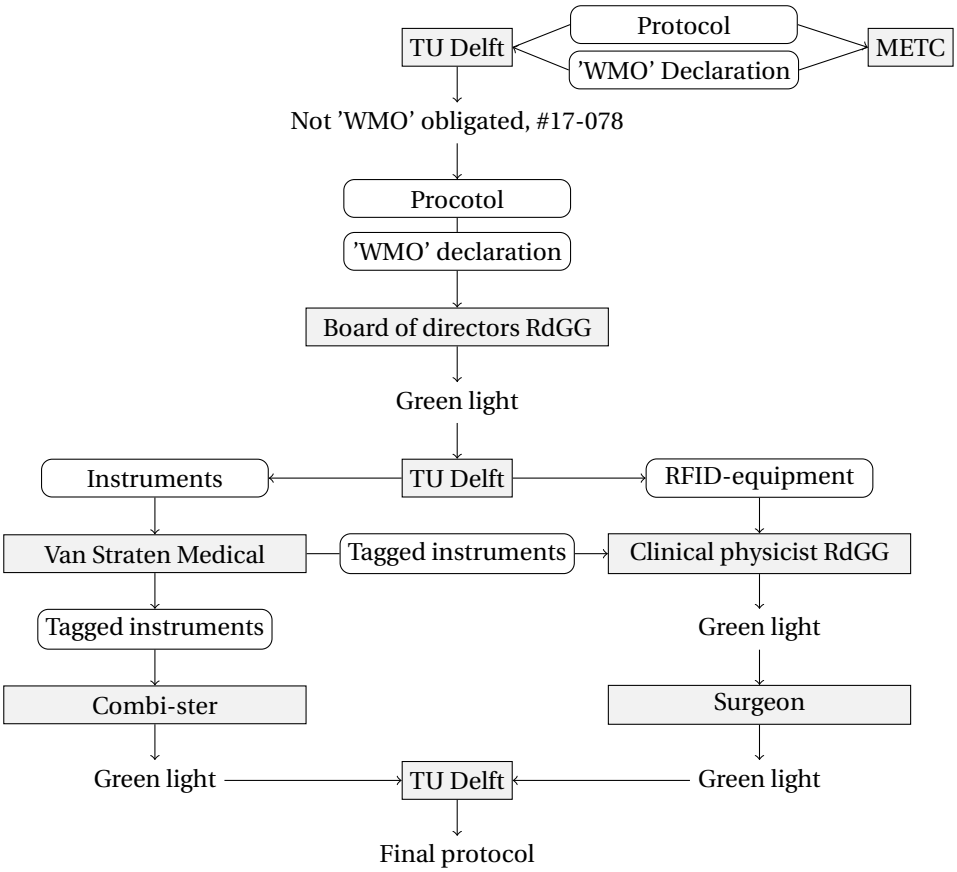

Figure 3.1: Overview of the acceptation process to finally perform in-vivo tests. The gray rectangles refer to parties or institutions, and the rounded white rectangles refer to concerned documents or objects.

3.2. WMO

A medical-scientific research protocol is subjected to the judgment of the Medische Ethische Toetsingscommissie (METC), which is an independent commission that is competent to declare whether research is within the scope of the Wet medisch-wetenschappelijk onderzoek met mensen (WMO).
Research is within the scope of the WMO when, as cited from [33]:

1. *It concerns medical/scientific research and*
2. *Participants are subject to procedures or are required to follow rules of behavior*

The METC Zuidwest Holland considered the RFID-research as proposed in this report to fall outside the scope of the WMO (METC-nr 17-079). Please refer to Appendix A for the documentation of the 'niet WMO-plichtig' declaration and the research protocol, as submitted to the METC.

According to [34], the proposed research must be submitted to the board of directors of the concerning institution. In the case of the RFID-research, the institution is the RdGG. The board of directors of RdGG did not object.

Since the RFID-research is not subjected to the WMO, reporting of in-vivo tests to the Inspectie Gezondheidszorg en Jeugd (IGJ) is not required. The IGJ is an independent ministerial inspectorate that protects and promotes the quality of healthcare.

3.3. Informed consent

The medical research ethics committees united (MEC-U) states that scientific research can be performed without permission from the patient when, as cited and translated from [34]:

- *Requesting permission for research is not reasonably possible or can be desired and the patients' privacy is guaranteed to be unharmed.*

And:

- *The research serves a common interest*
- *The research can not be performed without the concerning patient*
- *The patient did not object*

The RFID-research conflicts with the first three items, and therefore, permission from the concerned patient is required before conducting the in-vivo tests. This permission is granted through informed consent, which is presented to the patient prior to his/her surgery. The informed consent also discloses personal information. Please refer to Appendix B for the informed consent.

3.4. Electromagnetic interference

The literature shows conflicting results concerning Electromagnetic interference (EMI) of RFID-signals with surrounding medical devices. Christe et al. (2008) concluded that RFID-antennas did not cause performance alterations of surrounding equipment [35], while other studies showed that RFID-signals did interfere with surrounding equipment, leading to potentially harmful situations [36] [37]. According to Seidman et al. (2013), interference only occurred using certain frequency bands [38]. Most researchers encourage on-site interference-tests of RFID-signals with surrounding equipment prior to the installation of RFID-systems at the OR.

The antenna that operates at 2W is used for the RFID-setup. A radiated power of 2W results in an electric field strength of up to 300 V/m at the frontal area of the antenna, which is a factor one hundred higher than the norm value (3 V/m) under which medical equipment is guaranteed to function properly. The electric field strength is measured at an empty OR at RdGG using a PCE-EM 29 field strength meter (PCE Instruments UK Ltd., Southampton, UK). The latter observation is the reason that an EMI-test is performed.

The on-site EMI-test is performed at an OR of RdGG at location Voorburg. The RFID-antenna was activated and aimed at the anaesthesia workstation, patient monitoring system, syringe-pump and the electrosurgery hardware for one hour straight. The aforementioned equipment is considered most crucial to patient safety when malfunctioning due to EMI. The equipment was located within a 1.5-meter radius from the antenna and an electrical field strength of roughly 100 V/m was measured at this range. Furthermore, a patient simulator was connected to the patient monitoring system to simulate a real person's conditions. The electrosurgery machine was short-circuited through a resistor to mimic an in-vivo activation and the syringe pump was running at a rate of 10 mL/hour using a natriumchloride solution. The anaesthesia workstation was running a dummy program at which both oxygen and air were circulated. First signs of interference were expected at the electrocardiogram of the patient monitoring system since this feature is operating under very low signal strengths (± 1 mV). However, no interference was detected within the 1 hour of testing. Also, the patient monitoring system correctly alarmed when a tachycardia [1] (180bpm) was simulated using the patient simulator. Despite the exposure to electrical magnetic signals, the syringe pump functioned correctly at the pre-set flow of 10 mL/hour and the anaesthesia workstation did not show deviating performance. It was expected that reciprocal interference would occur between the electrosurgery machine and the RFID-antenna, leading to both malfunctioning of the electrosurgery machine and misdetection of RFID-tags within range of the antenna. Therefore, an RFID-tag was positioned in the detection range of the antenna while the use of electrosurgery was being imitated by short-circuiting the machine, see Figure 3.2. Both the electrosurgery machine and the RFID-antenna functioned properly.

The results of this EMI-test are considered positive by a clinical physicist of RdGG, who concluded that the RFID-system is *unlikely* to compromise patient safety.

Figure 3.2: Evaluating the occurrence of reciprocal interference between the electrosurgery device and the antenna. The antenna is facing towards the electrosurgery device and a tagged instrument is located within the detection range of the antenna while the use of electrosurgery was being imitated.

[1] A heart rate is considered a tachycardia when exceeding 100bpm

3.5. Sterilizability

The sterilizability of the tagged instruments is evaluated to conform to ISO standard 15883-1. The cleaning efficacy is assessed by the detection of residual proteinaceous contamination on the instruments. The results of the contamination test were in compliance with ISO standard 15883-1, and thus the cleaning efficacy is considered sufficient.

3.6. CE-marking

Referring to Council Directive 93/42/ EEC, concerning medical devices, Article 1 defines a medical device as follows [39]:

(a) 'medical device' means any instrument, apparatus, appliance, software, material or other article, whether used alone or in combination, including the software intended by its manufacturer to be used specifically for diagnostic and/or therapeutic purposes and necessary for its proper application, intended by the manufacturer to be used for human beings for the purpose of:

- *diagnosis, prevention, monitoring, treatment or alleviation of disease,*
- *diagnosis, monitoring, treatment, alleviation of or compensation for an injury or handicap,*
- *investigation, replacement or modification of the anatomy or of a physiological process,*
- *control of conception,*

and which does not achieve its principal intended action in or on the human body by pharmacological, immunological or metabolic means, but which may be assisted in its function by such means;

(b) 'accessory' means an article which whilst not being a device is intended specifically by its manufacturer to be used together with a device to enable it to be used in accordance with the use of the device intended by the manufacturer of the device;

As interpreted from the aforementioned directive, an attached RFID-tag is not intended to be used for diagnostic and/or therapeutic purposes, and therefore, is not considered a medical device. Also, the medical instruments are not being enabled by the RFID-tag. In fact, the intended use of the medical instrument is not affected by the tag. Therefore, the tag is also not considered an accessory to the instrument.

In conclusion, CE-marking is *not* required.

4

In-vivo tests

In the period from Oktober 2018 to January 2019, a total of 3 in-vivo tests were performed during different TEP-procedures at RdGG. A total of two tests were conducted at location Voorburg, and one at location Delft. During the pilot study, the position of the antenna was concluded to be acceptable, based on the detection ability and because no surgical actions were hindered. Hence, that position of the antenna is initially to be used during the first in-vivo test as well. The position of the antenna is adjusted in an iterative manner throughout the in-vivo tests, where the detection ability and the remarks from the surgeon are the main sources of feedback. As discussed in Section 3.3, this research is bound to informed consent. The informed consent (Appendix B) is signed by all patients that participated during the in-vivo tests.

4.1. Method

4.1.1. Test setup

The test setup for the in-vivo test is nearly identical to the test setup for the pilot study, as described in Section 2.1.3. The location of the surgeon(s), instrument table, and RFID-setup is presented in Figure 4.1. Note that the mayo stand is located in front of 'OR-assistant #1', and therefore not visible in the figure. The tasks are now distributed in such a way that both researchers are working on the data acquisition since the remaining tasks for the TEP-procedure are performed by the OR-personnel. The OR-personnel was not instructed to utilize the tagged instruments any differently.

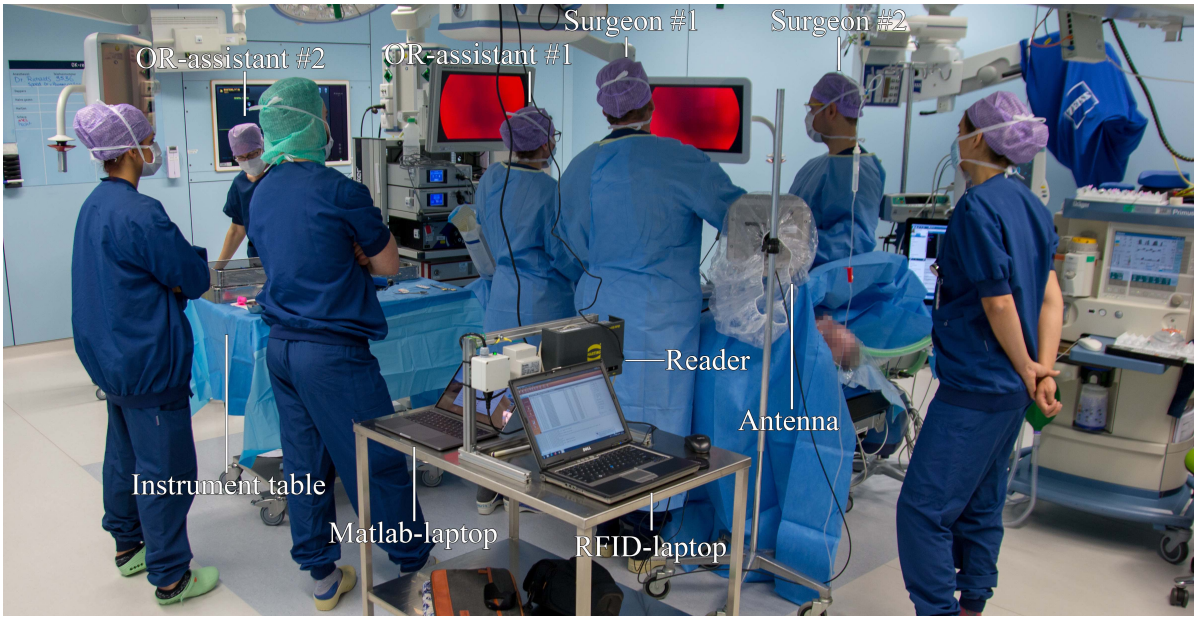

Figure 4.1: Test setup for the in-vivo tests, showing the location of the surgeon, instrument table, and RFID-setup.

4.1.2. Test procedure

When a TEP-procedure is planned where a test can be performed, Combi-ster is informed about the date and location. Combi-ster, which is the CSSD that is connected with RdGG, will make sure that the tagged instruments are provided to the correct OR. The informed consent is provided to the patient when he/she arrives at the holding, which is located at the OR-complex. As soon as the OR is available, the RFID-setup is installed. Both the RFID-software and the Matlab-script are launched, but not started. The antenna is not yet located next to the operating table in order to prevent scaring the patient and because it would hinder the anesthesiologists during the induction of the anesthesia. In consultation with the surgeon, the antenna is positioned at the desired location as soon as the induction is finished and the OR-assistants have set the surgical equipment. Then, both the RFID-software and the Matlab-script are started. The actual test takes place now, where the detected tags are registered within the RFID-software, and the actual instrument usage is manually registered by the researchers, using the Matlab-script. One researcher is always located next to the power supply of the RFID-setup to shut it down in case of malfunctioning or interference with surrounding equipment. After the surgery, the log files from both the RFID-software and the Matlab-script are saved and the test setup is removed from the OR before the patient emerges from anesthesia. The test is now completed and the instruments can be returned to Combi-ster for sterilization.

4.1.3. Data analysis

The data that is acquired through the in-vivo tests is transformed similarly as the data from the pilot study, see Section 2.1.5. The transformation of the data basically results in a time-based data set, containing an entry for each second since the start of the surgery, and showing the instruments that are detected at that moment. The data is validated using the Random Forest model that is generated during the pilot study (Section 2.2)

During the in-vivo tests, the surgeons appeared to be using slightly different instruments than assumed during the pilot study. The surgeons preferably used a plastic trocar instead of the metal 'Trocar 11mm' to function as a portal for the endoscope. Moreover, 'Trocar 11mm' appeared to be used during phase 3, instead of the 'Trocar 5mm #2', as a portal for a laparoscopic grasper, see Figure 4.2.

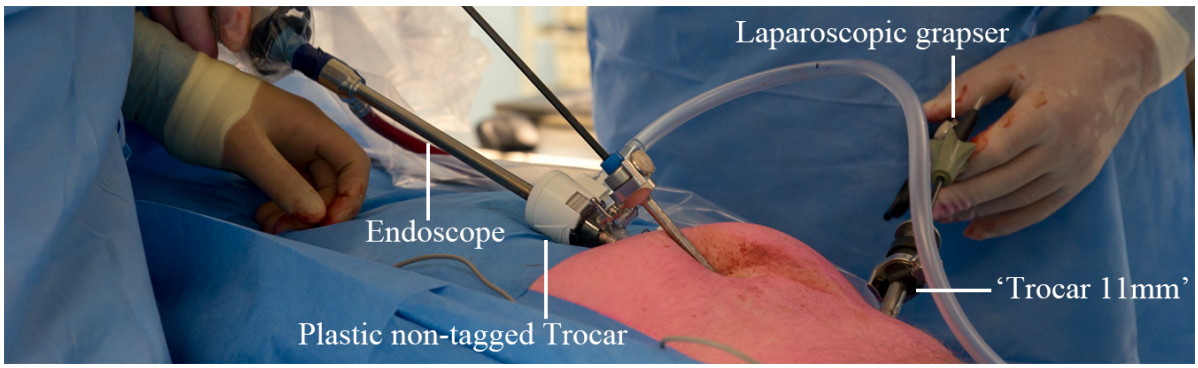

Figure 4.2: A plastic trocar is used instead of the tagged 'Trocar 11mm' as a portal for the endoscope. The 'Trocar 11mm' used during phase 3.

The transition from phase 1 to phase 2 of a TEP-procedure is, during the pilot study, assumed to be initiated by the insertion of 'Trocar 11mm', see Table 2.7. However, 'Trocar 11mm' is used at a different phase during the in-vivo tests and the plastic trocar is not taken into account during the measurement because it is not tagged. Thus, the plastic trocar can not initiate the transition between phase 1 and phase 2. Hence, problems arose when defining the actual phases of the manually annotated data. The endoscope is inserted through the plastic trocar as soon as the plastic trocar is positioned correctly through the abdominal wall and therefore, the definition of the phases is adapted in such a way that the endoscope now defines the transition between phase 1 and phase 2. The withdrawal of 'Trocar 11mm' from the surgical area contributes to the ending of phase 3. The adaptions to the initial phase definition from Table 2.7 are shown in Table 4.1.

Table 4.1: The four phases of a TEP-procedure, combined with instrument usage.

	Phase 1		**Phase 2**		**Phase 3**		**Phase 4**	
	Start	**Stop**	**Start**	**Stop**	**Start**	**Stop**	**Start**	**Stop**
1. Scalpel handle	in							
~~3. Trocar 11mm~~		~~in~~	~~in~~			~~out~~		
4. Endoscope		**in**	**in**			out		
5. Trocar 5mm #1						out		
6. Laparoscopic handle #1				in	in	out		
~~7. Trocar 5mm #2~~ **3. Trocar 11mm**						out		
8. Laparoscopic handle #2				in	in	out		
9. Electrosurgery cable						out		
10. Tweezer							in	out
11. Needle forceps							in	out

4.2. Results

The results of the three in-vivo tests are presented in this section. The results of the tests are presented separately to maintain overview. In the figures showing the results, for each instrument that was used during the test, a subplot is visible, and the x-axis displays the time of the surgery. A red rectangle represents the manually annotated data, and the blue dots refer to the moments of detection by the antenna. Note that for all tests, the 'Trocar 5mm #2' is not used. The tags that were attached to the instruments did not induce any discomfort to the surgeon. Also, no inconvenience was experienced due to the antenna that was located next to the surgeon. Figure 4.1 shows a cart on which the laptops and reader are located. This cart was not reported to obstruct any personnel movement.

4.2.1. Test 1

The first test was performed at location Delft and the total measurement took 31 minutes and 55 seconds. Several intra-operative complications arose during the TEP-procedure, forcing the surgeon to convert to open surgery. The measurement only includes the laparoscopic part of the procedure, since the instruments that are used during an open surgery are not equipped with tags. The 'Endoscope' is often detected, while the 'Laparoscopic handle #1', and the 'Needle forceps' are not detected throughout the test. Compared to the mimicked TEP-procedures during the pilot study, the 'Tweezer' is used more often during the first in-vivo test. The 'Laparoscopic handle #2' is detected without being registered as in use.

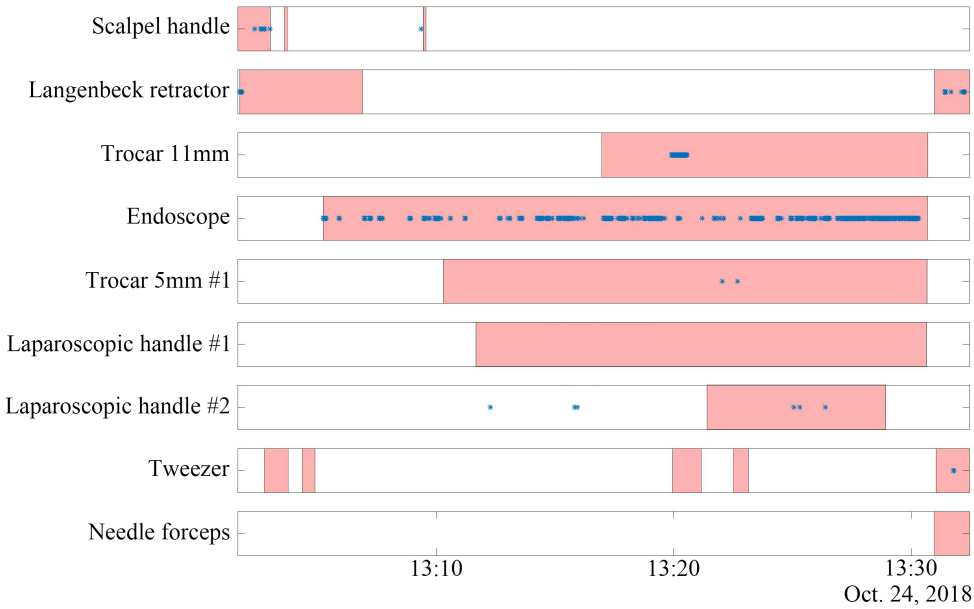

Figure 4.3: Raw data in-vivo test 1.

The accuracy of the predicted phases by the Random Forest model is 41.4%.

4.2.2. Test 2

The second test was performed at location Voorburg and had a duration of 11 minutes and 30 seconds. Both the tagged laparoscopic handles were not present in the set of instruments, due to complications in logistics. Also, the 'Trocar 5mm #1' is not used by the surgeon. The 'Endoscope', and 'Needle forceps' are not detected throughout the test, and the 'Langenbeck retractor' is detected while not being registered as in use.

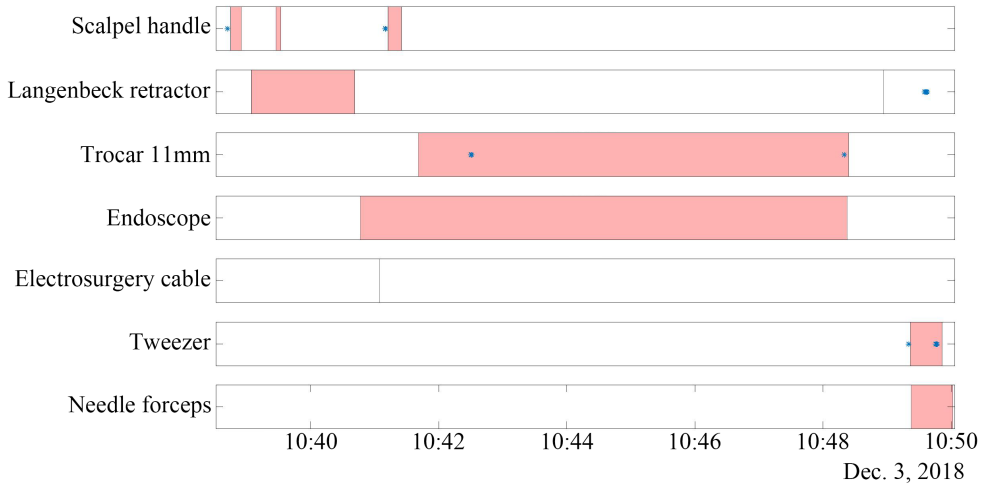

Figure 4.4: Raw data in-vivo test 2.

The gap in data due to the number of missing instruments made phase estimation not possible for this test.

4.2.3. Test 3

The third test was performed at location Voorburg and had a duration of 21 minutes and 33 seconds. Again, the 'Trocar 5mm #1' is not used by the surgeon. The 'Needle forceps' was not detected throughout the test. The 'Scalpel handle', the 'Langenbeck retractor', and the 'Endoscope' are detected while not being registered as in use.

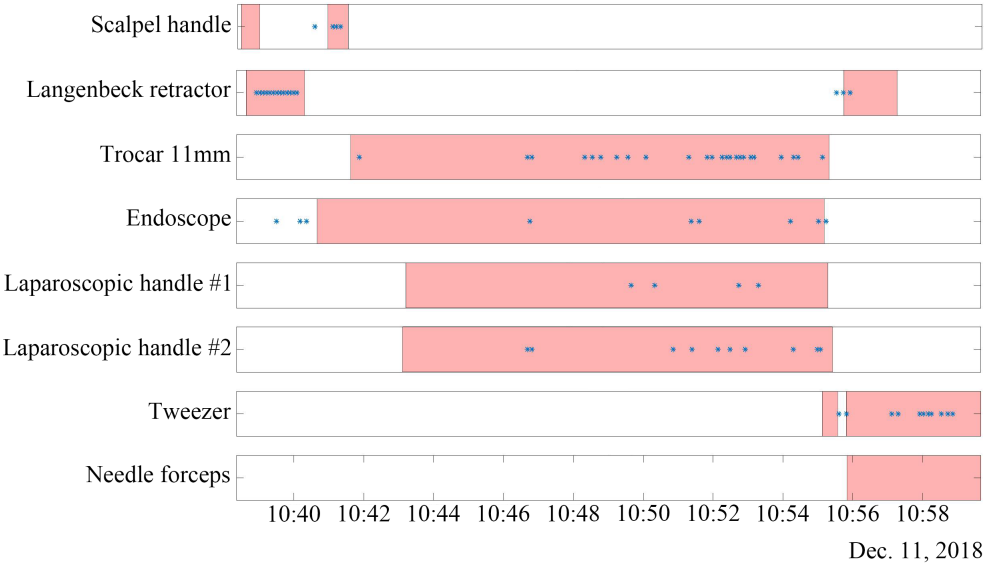

Figure 4.5: Raw data in-vivo test 3.

The accuracy of the predicted phases by the Random Forest model is 34.6%

4.3. Discussion in-vivo tests

This section will discuss the results of the three in-vivo tests that were performed to evaluate the applicability of an RFID-setup into a surgical environment. The tests were executed during TEP-procedures at RdGG, location Voorburg and Delft, using a selection of instruments that were equipped with tags. The applicability of the RFID-setup is evaluated based on three criteria: the compliance with regulations, the acceptance of the setup by OR-personnel, and the detection performance. Part III of this thesis will discuss the results in a broader context of the scope of this research.

An RFID-setup is presented that complies with the strict regulations for in-vivo research. The tags that are attached to the instruments do not affect the CE-marking. Also, the instruments that are equipped with tags are sterilizable conform to ISO standards. There is not yet a standard for electromagnetic radiation at the OR, but electromagnetic interference between the antenna and surrounding equipment can result in malfunctioning of equipment, which comprises patient safety. However, the radiation that is emitted by the antenna is evaluated by a clinical physicist to assess the risk of electromagnetic interference with surrounding equipment, and it was concluded that the RFID-setup is unlikely to compromise patient safety. The RFID-setup did not induce any discomfort to any of the OR-personnel during the tests.

The results of the three in-vivo tests indicate that detection of instruments is possible during actual surgeries, with the current RFID-setup. The majority of the detections are correct. A correct detection refers to an instrument being detected while actually being registered as 'in use'. The Figures of the results of the in-vivo tests (Figures 4.3, 4.4, and 4.5) are interpreted in such a way that correct detections occur within the registered actual usage of the instruments. This can be simplified to blue dots within the boundaries of the red rectangles. A selection of possible misdetections occurred. A misdetection is considered as a detection outside of the actual registered usage of the instruments. For example, during test 2 (Figure 4.4), the 'Langenbeck retractor' is detected at approximately 10:49:30, without being registered as 'in-use'. However, such detections can not directly be classified as misdetections, because a sometimes chaotic surgical environment could induce observation errors, where a very short usage of an instrument can occur unnoticed by the researchers. Also, detections that occurred close to the boundaries of the actual usage (e.g. Test 2, 'Scalpel handle', Figure 4.4), are considered inaccuracies in observing the instrument usage.

During the first test, the antenna was positioned similarly to the position of the antenna during the pilot study. However, the surgeon unexpectedly lowered the operating table, resulting in an area of detection of the antenna that did not align with the surgical area. Also, the surgeon encountered many complications during the first test. The effect of the complications on the instrument usage can possibly be derived from the extensive use of the Tweezer, see Figure 4.3. For the second test, the antenna was positioned lower, based on the feedback from the first test. The operating table was, however, altered to a slightly higher level than expected, causing the antenna to face partly against the leg of the patient. The RFID-setup as used in this study operates in the ultra high frequency (UHF) range. UHF RF-waves are absorbed by the liquids of the human body. Thus, the leg of the patient is expected to significantly inhibit the energy of the RF-waves, resulting in a poor detection ability, as seen in Figure 4.3. Given that the height of the operating table varies notably between surgeries, the position of the antenna was adapted accordingly during the third test; the antenna was positioned higher, while slightly inclined, facing towards the surgical area. This way, the alignment of the detection area of the antenna and the surgical area is presumed to be less susceptible to alterations in height of the operating table. This is assumed to explain the increased number of detections (Figure 4.5), compared to the second test (Figure 4.4).

The accuracy of the predicted phases by the Random Forest model is a measure of the extent to which the detection data can be used to predict the phase of surgeries. Note that the Random Forest model is based on the selection of instruments which is used during the pilot study. After the in-vivo tests, the selection of instruments used during surgery appeared to vary slightly from the instruments used during the pilot study, which was explained in Section 4.1.3. Hence, the Random Forest model is actually not directly applicable to assess the data of the in-vivo tests. It does, however, give an indication about the relevance of the data that is acquired through the current RFID-setup to predict the phases of surgeries. Based on the outcomes of the Random Forest model (overall accuracy of 38%), the detection ability of the RFID-setup is needed to be improved.

II

Attachment design

5

Introduction

5.1. Problem statement

Currently, the method of instrument identification as presented in Part I is solely applicable to Total Extraperitoneal Laparoscopic Hernia Repair (TEP), or similar procedures. One goal of this study is to make the method of instrument identification applicable to a broader range of surgeries. This requires that the method of instrument identifications is also evaluated during varying types of surgeries. Equipping all instruments that are used during the varying types of surgeries is considered infeasible at a research stage. Thus, the tags need to be interchangeable between instruments. However, the tags are currently attached using two stainless steel counterparts that fit around the instruments and are mostly fixated using a weld. The weld is considered a permanent fixation that cannot be dismantled by non-trained personnel or researchers, and thus requires the intervention of a surgical instrument maker. An example of an attachment to an instrument is presented in Figure 5.1. The tag is located on top of the attachment and encapsulated by a layer of epoxy to prevent damage to the tag during usage and the sterilization process. When the tag must be replaced (e.g. due to malfunctioning), the removal of the epoxy from the attachment requires a high effort and is likely to damage the attachment.

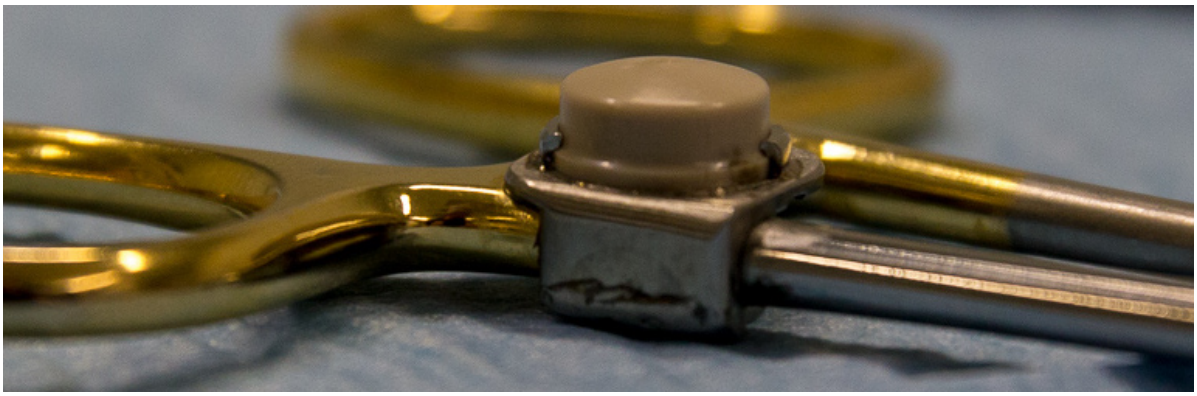

Figure 5.1: Original attachment of a tag to an instrument, showing two stainless steel counterparts welded together. The tag is encapsulated by epoxy to prevent damaging.

The aim of this design problem is thus:

Design an attachment to equip surgical instruments with tags in such a way that both the attachment and the tags are separately interchangeable between instruments without the need for any expertise.

5.2. Overview

The attachment is designed conform to a basic engineering design structure, as presented in Figure 5.2. A set of design requirements is defined based on the problem statement and regulatory aspects concerning patient safety. Based on the design requirements, a Computer-aided Design (CAD) is created. A prototype is then manufactured which is tested to conform to guidelines concerning patient safety. The test results provide feedback to the CAD, which is adapted accordingly; and to the design requirements, that are either adapter or complemented. The final solution is presented when all test results are positive and the design requirements are met.

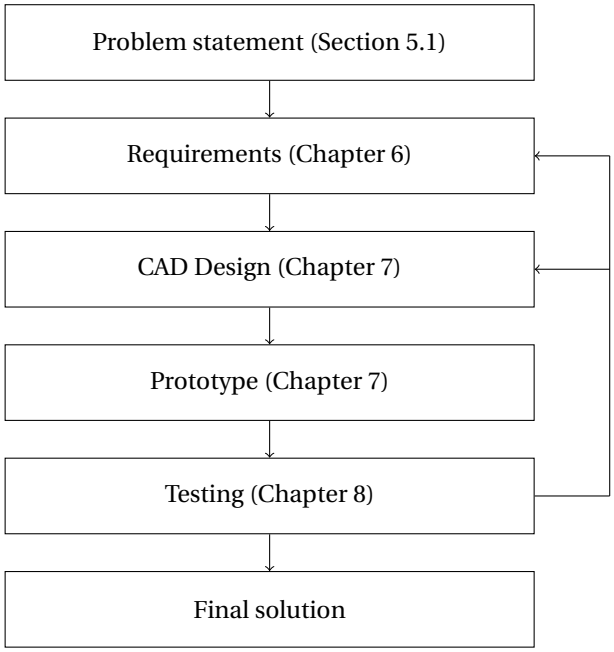

Figure 5.2: Design structure; A set of design requirements is defined based on the problem statement and regulatory aspects concerning patient safety. Based on the design requirements, a Computer-aided Design (CAD) is created. A prototype is then manufactured which is tested conform guidelines concerning patient safety. The test results provide feedback to the CAD, which is adapted accordingly; and to the design requirements, that are either adapter or complemented. The final solution is presented when all test results are positive and the design requirements are met.

Note that the design that is presented in this Part is not yet considered to be the final solution, but merely a proof-of-principle, including the test results during the n^{th} iteration through the design structure. After the design requirements are presented in Chapter 6, the design is presented in Chapter 7, followed by the test results in Chapter 8. The results are discussed in Chapter 9.

6

Design requirements

A list of design requirements is presented in Table 6.1. Note that the design requirements can be adapted or complemented according to the feedback from the test results during a sequence of iterations through the design structure . This study does not present the final solution of the design, and thus, the design requirements are not yet considered complete.

Since contact between the attachment and the instrument user or the patient undergoing surgery is unavoidable, the risk of tissue damage must be minimized. Therefore, the design of the attachment should have a smooth surface texture, while also preventing unnecessary sharp edges. The attachments are required to be sterile when used for surgeries. Therefore, the attachment should be autoclaveable[1] conform to guideline ISO 15.883-1. Since contact between the attachment and the patient undergoing surgery is likely to occur, the attachment must be biocompatible. As presented in Table 2.1, the tags are autoclavable. Thus, the attachment is not necessarily accountable for protecting the tags against the sterilization conditions. The tags that are used during this study are classified as on-metal tags, which requires them to be in contact with metal to function properly. Therefore, the tag must be affixed to metal, while taking into account that the reading distance of the tags deteriorates when enclosed by metal [29]. Instruments dropping on the floor is not inevitable. Thus, the attachments must be resistant to an impact with the floor from an assumed height of 1.5m. The Food and drug administration (FDA) roughly states that modified medical instruments, classified as 510(k), are required to be re-submitted for a CE-marking [40]. Thus, for the course of the research, the method of attaching the tag to the instrument must be designed in such a way that it classifies as an attachment, rather than a modification.

Table 6.1: Design requirements for the attachment of the RFID-tag to the instrument.

Geometry	- Rounded edges
Physical characteristics	- Autoclavable - Biocompatible - Smooth surface texture - The tag must be affixed to metal, but not enclosed by metal - Impact resistant (falling from 1.5m) - Attachment can be interchangeable between instruments
User requirements	- Attachment must not disturb usage of the instrument
Regulatory aspects	- Classifies as an attachment to the instrument, not as a modification to the instrument.

[1] Resistant to $130^{\circ}C$ and a pressure of 15psi.

7

Design description

7.1. Computer-aided Design

A design is presented that enables the equipment of tags to instruments. The design consists of two counterparts that fit around an instrument. The upper- and lower part of the design are fixed around the instrument using a clip on each corner of the design. Unfixing the upper part from the lower part is done by firmly pressing the four pins towards the center of the design. The clips are designed in such a way that the upper- and lower part of the design are difficult to be separated without the use of a tool to exert a force on the four clips simultaneously. This prevents the design from being dismantled too easily. Originally, the tag was encapsulated by an epoxy on top of the attachment. Given that the tags that are used during this study are all autoclavable, the epoxy only serves as protection against impacts. The newly introduced attachment is designed in such a way that the tag is located inside the attachment, which protects the tag, and excludes the necessity for an epoxy. The CAD is created using SolidWorks (Dassault Systèmes, Vélizy-Villacoublay, France). The CAD in Figure 7.3 shows the design in the closed position (7.1a) and the open position (7.1b). The outer dimensions are shown in Figure 7.2. The design is based on a Xerafy Dot XXS (Xerafy, Singapore, Singapore) tag being located within it, because the Xerafy Dot XXS is the smallest tag from the selection of tags used in this study, and no direct difference in performance is noticed between the tags. Nevertheless, the design is easily adaptable to varying types of tags. However, this will increase the dimensions of the designed attachment.

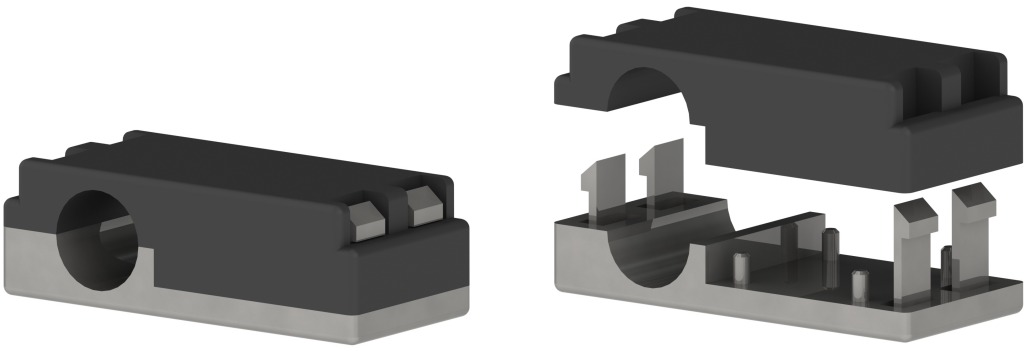

(a) Design closed.

(b) Design open.

Figure 7.1: Attachment design.

Figure 7.3a shows the tag equipped to an imaginary instrument with a shaft of ⌀3.2mm (e.g. surgical scissor). The design is easily applicable to varying types of instruments by adapting the dimension and shape of the extrusion through which the instrument shaft fits. The outer dimensions of the attachment then change accordingly. For instance, the length of the attachment can be formulated as $l = 10.6 + \varnothing_{\text{shaft}}$ [mm]. Figure 7.3b shows the location of the tag inside the attachment. This way, the position of the tag is fixed, and protected against damage, without the use of an epoxy. Due to the absence of an epoxy, the tag can be replaced without removing the epoxy first, which prevents damaging the attachment.

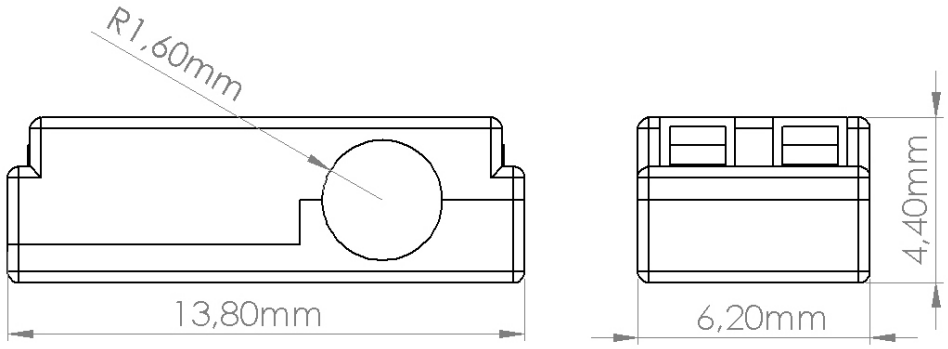

Figure 7.2: Outer dimensions of the design.

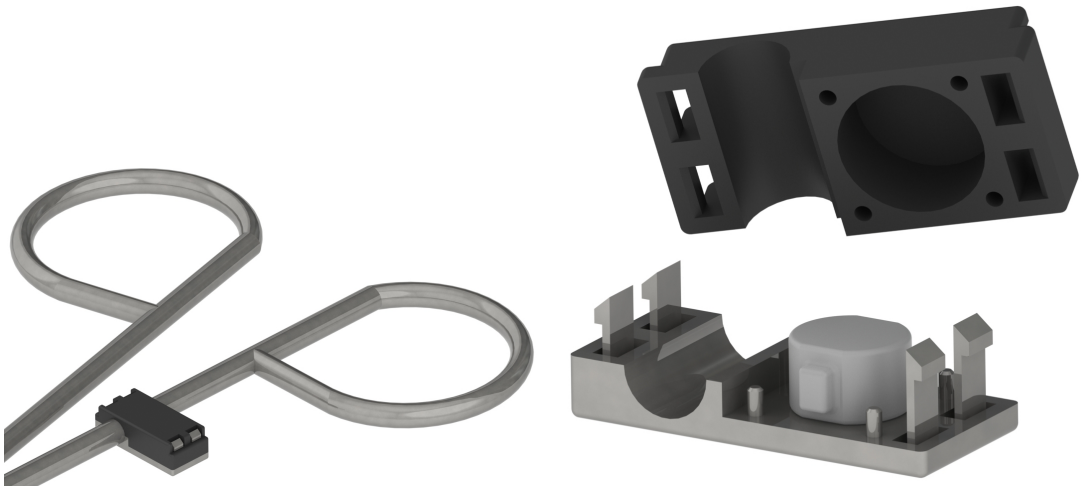

(a) A tag equipped to an imaginary instrument.

(b) The position of a tag inside the attachment.

Figure 7.3: Usage of the attachment.

7.2. Manufactured design

Figure 7.4 shows the prototype that is manufactured conform the CAD in the Dienst Elektronische en Mechanische Ontwikkeling (DEMO)-lab at the TU Delft. The lower part of the design is made out of stainless steel using a Mysing 100 PM 3D metal printer (SISMA S.p.A., Vicenza, Italy) since the tags are specified as affixed to metal. The upper part, however, is made out of R5/R11 plastic, because the performance of the tag is known to deteriorate when being enclosed by metal. The upper part is manufactured using an EnvisionTEC 3D printer (ENVISIONTEC, INC., Dearborn, USA).

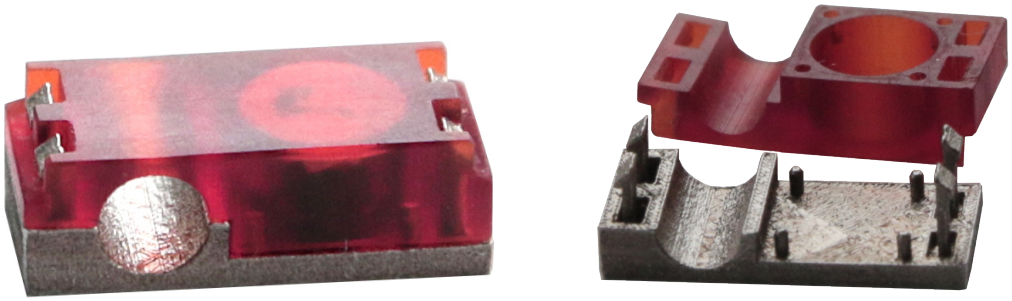

(a) Manufactured design closed.

(b) Manufactured design open.

Figure 7.4: Manufactured design.

8 Testing

8.1. Detection ability

During the detection ability test, it is evaluated to what extent the designed attachment affects the detection ability of a tag that is located within it.

8.1.1. Test procedure

The performance of a tag inside the designed attachment is compared to the performance of a tag that is fixed to a test plate. The test plate, as shown in Figure 8.1 originates from the research performed by [29], and is considered a reference attachment. The test plate is manufactured using the same material as the bottom part of the designed attachment (316L stainless steel). The tag that is used is a Xerafy Dot XXS (Xerafy, Singapore, Singapore), see Table 2.1 for the specifications.

Figure 8.1: Designed attachment, compared to a test plate.

The test is performed in a lab at the TUD, using the RFID-setup as provided in this study. The antenna is positioned upright on a table, and both the reader and RFID-laptop are located behind the antenna. The table itself is provided with a distance reference that begins at the frontal area of the antenna, see Figure 8.2. A single run consists of the following consecutive steps, where a surgical scissor is equipped with a tag that is fixed to the test plate:

1. Scissor is located in line with the center of the antenna, at a distance of 1 meter, while the tag is facing towards the antenna.
2. Scissor is slowly being displaced towards the antenna.
3. As soon as the tag is detected by the antenna, the current distance 'X' (see Figure 8.2) is noted.

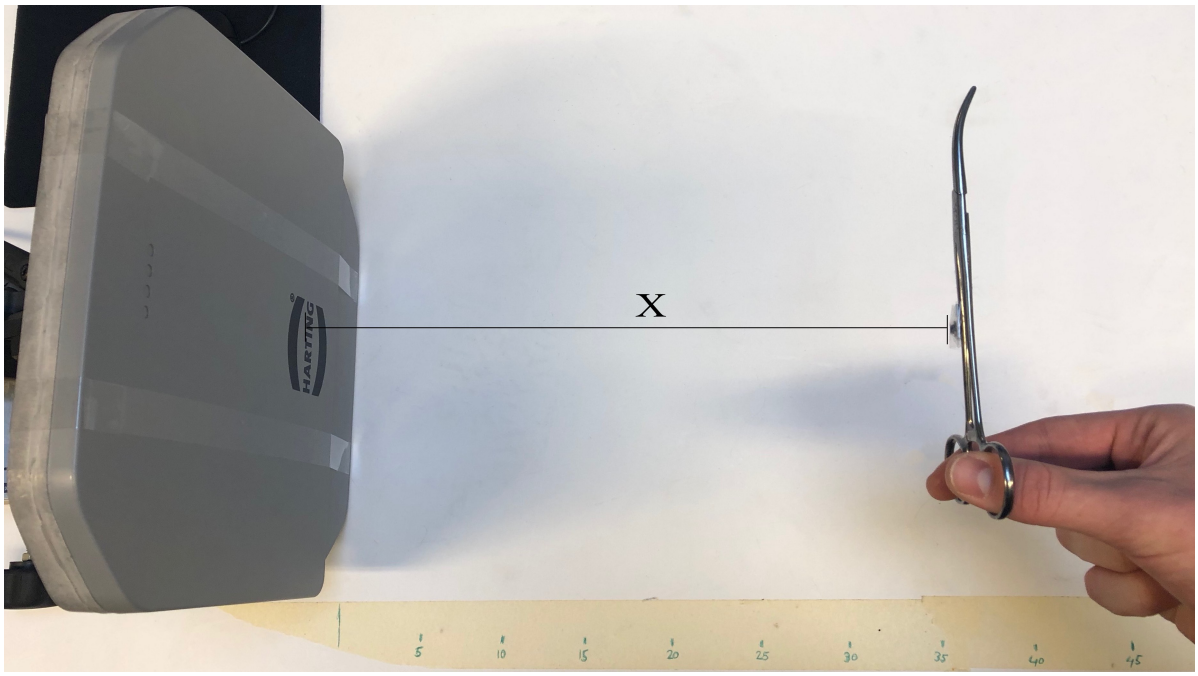

Figure 8.2: Setup to test the detection ability of the tag in the attachment design.

These steps are repeated an additional 19 times, resulting in a total of 20 runs. These 20 runs are in turn repeated with the following configurations:

- Scissor + test plate + tag, while tag facing away from the antenna.
- Scissor + designed attachment + tag, while tag facing towards the antenna.
- Scissor + designed attachment + tag, while tag facing away from the antenna.

Resulting in a total of 4x20 runs that are performed.

8.1.2. Results

The resulting detection distances 'X' are presented in Table 8.1, where two columns refer to the configuration where the tag faces towards the antenna, and two columns to the configuration where the tag faces away from the antenna.

Table 8.1: Detection ability test results.

	Tag facing towards antenna		Tag facing away from antenna	
Run No.	$X_{\text{Test plate}}$ [cm]	$X_{\text{Designed attachment}}$ [cm]	$X_{\text{Test plate}}$ [cm]	$X_{\text{Designed attachment}}$ [cm]
1	40	45	35	35
2	40	50	30	35
3	40	50	30	45
4	35	50	35	45
5	35	50	35	50
6	35	50	30	45
7	35	50	35	50
8	35	50	35	50
9	40	50	35	45
10	35	50	35	45
11	35	50	35	40
12	35	50	35	45
13	35	50	35	50
14	35	50	30	50
15	35	50	30	35
16	30	55	35	45
17	35	50	30	45
18	35	50	30	45
19	35	50	30	50
20	25	50	35	45
Average →	**35.25**	**50**	**33**	**44.75**

8.2. Sterilizability

The designed attachment is inspected by Combi-ster, the external CSSD-department of RdGG; and a Deskundige Steriele Medische Hulpmiddelen (DSMH) from RdGG. The upper part of the attachment design is currently prototyped out of R5/R11 plastic, which is a non-autoclavable material. Hence, the design could not yet be evaluated on the sterilizability using conventional methods that involve the autoclave. Thus, in this case, a visual examination of the design by experts is executed. The attachment is not expected to enter the human body during surgery. However, contamination of the attachment is likely to occur, for example, due to contact with blood on the surgical gloves. And thus, the judgment on sterilizability is based on the worst case scenario where the design is completely submerged into a proteinaceous fluid (e.g. blood).

The necessity of a new attachment design was acknowledged during the meeting, and the proposed design was concluded to enable interchangeability of the tags between different instruments. The rounded edges of the design will most likely not induce any risk of damaging human tissue. The possibility was addressed that contamination could gather inside the cavities at the four corners where the pins fixate the upper part to the lower part. Such a cavity is encircled in Figure 8.3. Also, the use of different materials for the upper- and lower part of the design might result in a different deformation of the materials when being exposed to the high temperatures of an autoclave. The effect that the varying deformations might have on the seamlessness between the contact area of the upper- and lower part of the design is yet unknown. The remarks about the cavities and the use of two different materials are rather advisory for further development than bottlenecks that would cause a rejection of the design.

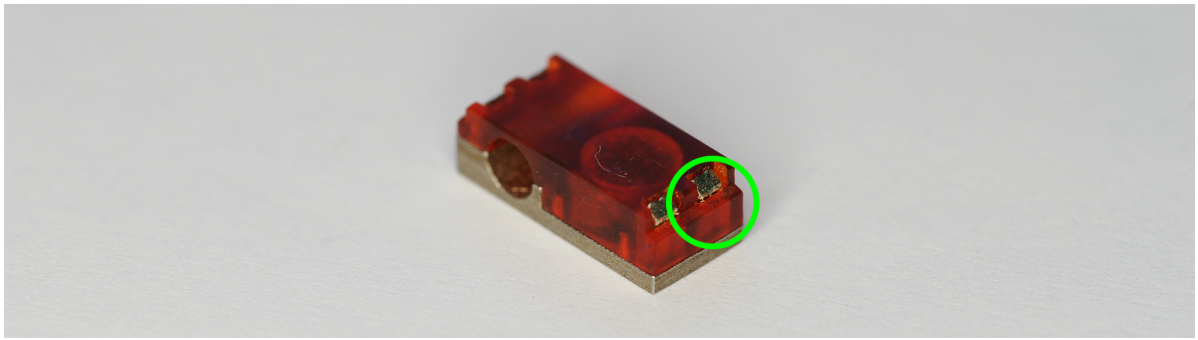

Figure 8.3: Cavity at the corner of the design in which contamination could gather.

9

Discussion attachment design

This section discusses the method of equipping instruments with tags in such a way that both the attachment and the tags are separately interchangeable between instruments. An attachment is designed conform a basic engineering design structure. The tag can be located within the attachment, without the need for epoxy to protect the tag against damage and the sterilization process.

The designed attachment is evaluated on detectability and sterilizability. Derived from the results as presented in Section 8.1, a tag that is located inside the designed attachment performs better than a tag that is fixed to a test plate that served as reference. The detection ability slightly deteriorated when the tag was facing away from the antenna, which is likely to occur because the RF-waves reach the tag by conduction through the metal, instead of directly. The test setup was not comparable to a surgical setting due to a selection of assumed factors: the researcher was not wearing surgical gloves, allowing for detuning of the RF-waves; the table deflects the radiated RF-waves from the antenna; no surrounding surgical devices; and only a single person in the room, compared to a greater amount of people present in a surgical setting. Thus, the results from the detection ability test are inconclusive about the applicability of the designed attachment into a surgical setting. However, the results indicate that the designed attachment does not deteriorate the detection performance of tags compared to a reference test plate. The designed attachment does not require modifications to the instruments to which it will be attached, and it also not considered to be an accessory to the instrument. Thus, the CE-mark is most likely to be retained.

The tags that are used during the detection ability test (Xerafy Dot XXS) are specified as being affixed to metal. The level of pressure between the tag and metal appeared to significantly affect the detection ability of the tag. Prior to the detection ability test, there appeared to be a narrow space between the top of the tag and the upper part (plastic) of the designed attachment. Hence, the tag was not firmly pressed against the bottom part (metal) of the designed attachment, which resulted in a maximum detection distance of approximately 5cm. Thus, a layer of plastic had to be applied on the tag to compensate for the narrow space between the top of the tag and the upper part of the designed attachment. The surface of the test plate, as presented in Figure 8.1, appears to be rough, and the pressure between the tag and the test plate is considered sufficient due to the tape. Although the specifications about the tag do not mention the area of contact with metal, it is expected that the roughness of the test plate's surface explains the difference in performance with the designed attachment.

The RF-waves are assumed to propagate freely through the plastic upper part of the designed attachment. The designed attachment is unlikely to disturb the usage of the instrument, due to the dimensions of the attachment. The lower part is made out of stainless steel 316L, which is often used for surgical instruments, and thus considered a biocompatible, and autoclavable material. The upper part, however, is made out of R5/R11 plastic, which is not considered autoclavable. Thus, the material of the upper part of the final design is yet to be selected in further research. The strength of the designed attachment is yet to be evaluated by means of a controlled impact to simulate a drop on the floor. A proposed method to realize such an impact is presented in Appendix E.

III

General discussion & conclusion

Discussion

This thesis evaluates the applicability of RFID-technology into a surgical setting to identify instruments during a TEP-procedure. A pilot study is executed in a near-surgical setting to evaluate the applicability of an off-the-shelf RFID-setup into a surgical setting. The applicability is assessed on acceptance by the operating room personnel, regulatory aspects to perform in-vivo tests, and performance. The results of the pilot study are incorporated into the process of realizing in-vivo testing, which involves compliance with a selection of regulations and standards. Once in-vivo testing was approved, a selection of in-vivo tests was executed to evaluate the applicability of the RFID-setup in a real surgical setting. Moreover, a first step has been taken to extend the research to a greater range of surgery types.

An RFID-setup is presented that has shown the ability to correctly identify instruments during surgery when being used by the surgeon. The RFID-setup and testing method comply with all necessary regulations to perform in-vivo testing, and no discomfort or obstruction was experienced due to the RFID-setup by the OR-personnel and the surgeon. The latter is of great importance to ensure future testing. There is no direct relation found during the in-vivo tests between the detection ability of an instrument and the type of tag that is equipped to it. Factors, such as the presence of a human body in front of the antenna that can absorb the RF-waves, are however assumed to affect the detection ability. The positioning of the antenna is thus deemed crucial. An overall phase estimation accuracy of 38% is achieved using a Random Forest model with data from the in-vivo tests. Although this accuracy is not completely reliable, the detection ability of the RFID-setup is yet to be improved in order to be suitable for phase recognition models to provide information on the progress of surgeries to the OR-schedulers. No conclusions can be drawn yet on the effect of electrosurgery on the detection ability during surgeries because no electrosurgery was used during the in-vivo tests. However, the electromagnetic interference test from Section 3.4 did not result in a noticeable interference with the antenna during electrosurgery activations. A designed attachment is presented that enables the equipment of tags to instruments in such a way that both the attachment and the tags are separately interchangeable between instruments without the need for any expertise. The prototype is manufactured, evaluated on detection ability, and judged on sterilizability. The designed attachment does not deteriorate the detection of a tag that is located within it, and advice on sterilizability is presented for future development of the design. The advice is incorporated into the recommendations for future research.

Similar research is performed by [20], who aims at automatically recognizing the surgical workflow using a selection of multiple RFID-antennas to locate instruments. An overall detection rate of 92% is reported of instruments at the operating table and the instrument table. However, their research is performed at an empty OR and there is no indication found on how the accuracy is calculated. The results of this thesis indicate that the detection ability of an RFID-setup deteriorates when applied in a real surgical setting during surgeries. Factors such as the presence of a patient on the operating table are assumed to affect the propagation of RF-waves, and thus, the location of the antenna is deemed crucial. Though, the fusion of data from multiple antennas might improve the detection ability of instruments during surgeries. Work from Japan [41] presents one of the few studies that performed in-vivo tests using RFID, where a setup is used that can successfully detect instruments during surgery. Their main objective of instrument identification is however aimed at counting the instrument usage to prevent instrument breakage and retention of instruments. Thus, they located their antenna beneath a mayo stand, because frequently used instruments are often placed on it during surgery. The aim of their study deviates somewhat from the aim of this thesis, but it does, however, highlights the additional, and promising applications of RFID in a surgical setting. Once the utilization rate of instruments can be tracked, the CSSD can efficiently identify defective instruments [42], and it allows for maintenance scheduling [43]. A discussion was held with the OR-personnel after the first in-vivo test about their opinion on the applicability of the RFID-technology as applied in this thesis. The previously mentioned applications of RFID were acknowledged as additional advantages when applying RFID to track instrument usage. Lastly, according to [43], archiving of instruments usage minimizes the “risk associated with cross-contamination of certain diseases that are not yet completely understood. An example of the latter is the need to remove any instrument that has ever been in contact with a patient who presumably has Creutzfeldt-Jakob disease from further use”. Adding to the research found in the literature, this thesis provides new insights about the applicability of an RFID-setup in a real surgical setting to identify the usage of instruments, while aiming at providing information on the progress of ongoing surgeries.

Limitations

The number of performed in-vivo tests is limited, as just a single set of instruments is equipped with tags. Despite the fact that a selection of TEP-procedures is often scheduled consecutively on one day, the utilization rate of the tagged instruments is limited to once a day, as sterilization of the instruments is required after each in-vivo test. Thus, the potential amount of in-vivo data that could have been acquired decreased significantly, causing the evaluation of the detection ability to be based on limited results. Also, the Random Forest model is therefore necessarily based on a simulated set of data from the pilot study that includes several assumptions, such as the time required to insert a trocar. As the selection of instruments that was used during the in-vivo tests varied slightly from the instruments that were used during the pilot study, there is a gap in data, and thus, the results from the Random Forest model are less reliable for phase recognition during real TEP-procedures. Furthermore, the tags are considered applicable to the selection of TEP-instruments. However, the current tags are unlikely to fit onto small instruments as used during neurosurgery for example [41].

Future work

The limited number of performed in-vivo tests emphasizes the necessity of an attachment that can provide instruments with tags without needing the intervention of a surgical instrument maker. Hence, the attachment as designed in this thesis needs to be further developed. The next step of the design process is to select a material for the upper part, after which conventional sterilization tests and strength tests can be performed. The positioning of the antenna is repeatedly been considered to significantly affect the detection ability of the RFID-setup throughout this thesis. Continuation of this research should, therefore, focus on the position of the antenna during in-vivo tests to improve the detection ability. The detection area of the antenna needs to be independent of the operating table height; and the position of patient, OR-personnel, and surgeon. The Random Forest model is able to estimate the phases based on the instrument usage data. However, such a model needs to be trained based on in-vivo data instead of data from the pilot study, in order to obtain more reliable results. Eventually, information about the progress of ongoing surgeries must be automatically presented to the OR-schedulers. This does, however, needs the phase estimation to be continuously executed during surgeries. Appendix F provides a preliminary application proposal to estimate the phase of ongoing surgeries in 'real-time'.

Conclusion

This thesis evaluates the applicability of an RFID-setup into a surgical setting to identify instruments when being used by the surgeon. The setup has shown the ability to identify instruments that are equipped with RFID-tags. All regulations to perform in-vivo tests are complied with, and no discomfort of the RFID-setup is experienced by the surgeon and OR-personnel during in-vivo tests. Hence, future in-vivo testing is warranted to optimize the setup. A Random Forest model can estimate the phases of ongoing surgeries, based on instrument usage data that is acquired through an RFID-setup. The current setup, however, needs to be optimized to improve the detection ability. So far, the first step to make the method of instrument identification applicable to a broader range of surgeries has resulted in a prototyped attachment design to equip instruments with RFID-tags. The attachment is designed in such a way that both the attachment and the RFID-tags are interchangeable between instruments. Further development is needed for the design to comply with a selection of regulations to perform in-vivo testing.

Bibliography

[1] Florent Lalys and Pierre Jannin. Surgical process modelling: a review. *International Journal of Computer Assisted Radiology and Surgery*, 9(3):495–511, May 2014.

[2] Fabian van Luyn. Intra-operative estimation of surgical progress. Master's thesis, Technical University Delft, 2017.

[3] van Kranenburg R. Ward, M. Rfid: Frequency, standards, adoption and innovation. 2006.

[4] Brecht Cardoen, Erik Demeulemeester, and Jeroen Beliën. Operating room planning and scheduling : A literature review. *European Journal of Operational Research*, 201(3):921–932, 2010.

[5] MD MBA Macario, Alex, MD Vitez, Terry, BA Dunn, Brian, and MD McDonald, Tom. Where Are the Costs in Perioperative Care?: Analysis of Hospital Costs and Charges for Inpatient Surgical Care. *Anesthesiology: The Journal of the American Society of Anesthesiologists*, 83(6):1138–1144, 12 1995.

[6] Atidel B Hadj and Pierre Ladet. Operating rooms scheduling. 99:52–62, 2006.

[7] Annetje C.P. Guédon, M. Paalvast, F. C. Meeuwsen, D. M.J. Tax, A. P. van Dijke, L. S.G.L. Wauben, M. van der Elst, J. Dankelman, and J. J. van den Dobbelsteen. 'It is Time to Prepare the Next patient' Real-Time Prediction of Procedure Duration in Laparoscopic Cholecystectomies. *Journal of Medical Systems*, 40(12):4–9, 2016.

[8] Daiki Min and Yuehwern Yih. An elective surgery scheduling problem considering patient priority. *Computers and Operation Research*, 37(6):1091–1099, 2010.

[9] R Jonnalagadda, E R Walrond, S Hariharan, M Walrond, and C Prasad. Evaluation of the reasons for cancellations and delays of surgical procedures in a developing country. (June):716–720, 2005.

[10] S. Ayca Erdogan and Brian T. Denton. *Surgery Planning and Scheduling*. American Cancer Society, 2011.

[11] Thomas Neumuth and Oliver Burgert. Surgical workflow, methods and applications. *Asian hospital healthcare management*.

[12] Andru P Twinanda, Sherif Shehata, Didier Mutter, Jacques Marescaux, Michel De Mathelin, and Nicolas Padoy. EndoNet : A Deep Architecture for Recognition Tasks on Laparoscopic Videos. 36(1):86–97, 2017.

[13] Atsushi Nara, Kiyoshi Izumi, Hiroshi Iseki, Takashi Suzuki, Kyojiro Nambu, and Yasuo Sakurai. Surgical workflow monitoring based on trajectory data mining. In Takashi Onada, Daisuke Bekki, and Eric McCready, editors, *New Frontiers in Artificial Intelligence*, pages 283–291, Berlin, Heidelberg, 2011. Springer Berlin Heidelberg.

[14] A. James, D. Vieira, B. Lo, A. Darzi, and G. Z. Yang. Eye-gaze driven surgical workflow segmentation. In Nicholas Ayache, Sébastien Ourselin, and Anthony Maeder, editors, *Medical Image Computing and Computer-Assisted Intervention – MICCAI 2007*, pages 110–117, Berlin, Heidelberg, 2007. Springer Berlin Heidelberg.

[15] Ralf Stauder, Asli Okur, Nassir Navab, Armin Schneider, and Hubertus Feu. Detecting and analyzing the surgical workflow to aid human and robotic scrub nurses. In *CURAC*, 2014.

[16] David Bouget, Max Allan, Danail Stoyanov, and Pierre Jannin. Vision-based and marker-less surgical tool detection and tracking: a review of the literature. *Medical Image Analysis*, 35:633–654, 2017.

[17] Lin Zhang, Menglong Ye, Po Ling Chan, and Guang Zhong Yang. Real-time surgical tool tracking and pose estimation using a hybrid cylindrical marker. *International Journal of Computer Assisted Radiology and Surgery*, 12(6):921–930, 2017.

[18] N. Alberto Borghese and I. Frosio. Compact tracking of surgical instruments through structured markers. *Medical and Biological Engineering and Computing*, 51(7):823–833, 2013.

[19] Fahed Elsamnah and Wahju Sediono. Medical navigation based on coloured markers for image-guided surgery. *Procedia Computer Science*, 42(C):138–144, 2014.

[20] C. Meißner and T. Neumuth. RFID-based surgical instrument detection using Hidden Markov models. *Biomedical Engineering / Biomedizinische Technik*, 57(SI-1 Track-H):689–692, 2012.

[21] J. Koffeman. Real-time surgical phase recognition based on identification of medical instruments at the operation room (literature thesis). 2018.

[22] Kazuhiko Yamashita, Kaori Kusuda, Yoshitomo Ito, Masaru Komino, Kiyohito Tanaka, Satoru Kurokawa, Michitaka Ameya, Daiji Eba, Ken Masamune, Yoshihiro Muragaki, Yuji Ohta, Chugo Rinoie, Kenji Yamada, and Yoshiki Sawa. Evaluation of surgical instruments with radiofrequency identification tags in the operating room. *Surgical Innovation*, 25(4):374–379, 2018. PMID: 29716450.

[23] R. Weinstein. Rfid: a technical overview and its application to the enterprise. *IT Professional*, 7(3):27–33, May 2005.

[24] McCormack K Fraser C Vale L Perez J Wake, BL and A Grant. Transabdominal pre-peritoneal (tapp) vs totally extraperitoneal (tep) laparoscopic techniques for inguinal hernia repair. *Cochrane Database of Systematic Reviews*, (1), 2005.

[25] Robert J. Fitzgibbons and R. Armour Forse. Groin hernias in adults. *New England Journal of Medicine*, 372(8):756–763, 2015. PMID: 25693015.

[26] Med-info. Operatieverslag: Correctie hernia inguinalis (liesbreuk).

[27] Wellkang Tech Consulting. What is ce marking (ce mark).

[28] Robert DiPietro, Ralf Stauder, Ergün Kayis, Armin Schneider, Michael Kranzfelder, Hubertus Feußner, Gregory D. Hager, and Nassir Navab. Automated Surgical-Phase Recognition Using Rapidly-Deployable Sensors. *M2CAI workshop, MICCAI, Munich*, 2016.

[29] Mariëlle Haring. Instrument tracking in the operating room, optimization of rfid tag performance. Master's thesis, Technical University Delft.

[30] Scikit-learn. 3.2.4.3.1. sklearn.ensemble.randomforestclassifier.

[31] L. Breiman. Random forests. 2001.

[32] Scikit-learn. Decision trees.

[33] Centrale Commissie Mensgebonden Onderzoek (CCMO). Your reserach: does it fall under the wmo.

[34] Medical Research Ethics Committees United. Niet wmo plichtig onderzoek.

[35] Gregg Maggioli Dustin Doty Robert Frye Barbara Christe, Elaine Cooney and Jason Short. Testing potential interference with rfid usage in the patient care environment. 2008.

[36] Hensbroek R Beinat E Binnekade JM Bakker PJ Togt R van der, van Lieshout EJ. Electromagnetic interference from radio frequency identification inducing potentially hazardous incidents in critical care medical equipment. 2009.

[37] Webster CS Merry AF Houliston B, Parry D. Interference with the operation of medical devices resulting from the use of radio frequency identification technology. 2009.

[38] Joshua W Guag Seth J Seidman. Adhoc electromagnetic compatibility testing of non-implantable medical devices and radio frequency identification. 2013.

[39] Council of the European Union. *COUNCIL DIRECTIVE 93/42/EEC*.

[40] FDA. *Deciding When to Submit a 510(k) for a Change to an Existing Device*. U.S. Department of Health and Human Services, 2017.

[41] Kazuhiko Yamashita, Kaori Kusuda, Yoshitomo Ito, Masaru Komino, Kiyohito Tanaka, Satoru Kurokawa, Michitaka Ameya, Daiji Eba, Ken Masamune, Yoshihiro Muragaki, Yuji Ohta, Chugo Rinoie, Kenji Yamada, and Yoshiki Sawa. Evaluation of Surgical Instruments With Radiofrequency Identification Tags in the Operating Room. *Surgical Innovation*, 25(4):374–379, 2018.

[42] Kaori Kusuda, Kazuhiko Yamashita, Akiko Ohnishi, Kiyohito Tanaka, Masaru Komino, Hiroshi Honda, Shinichi Tanaka, Takashi Okubo, Julien Tripette, and Yuji Ohta. Management of surgical instruments with radio frequency identification tags: A 27-month in hospital trial. *International Journal of Health Care Quality Assurance*, 29(2):236–247, 2016. PMID: 26959900.

[43] Yannick Meiller, Sylvain Bureau, Wei Zhou, and Selwyn Piramuthu. RFID-embedded decision support for tracking surgical equipment. *Proceedings of the Annual Hawaii International Conference on System Sciences*, pages 1–6, 2011.

[44] Wireshark Foundation. Wireshark - go deep.

[45] KimiNewt. Pyshark.

Appendix

A

WMO approvals

A.1. Not WMO

METC Zuidwest Holland

TU Delft
Department of BioNechanical Engineering
T.a.v. mw. F.C. Meeuwsen, MD
Mekelweg 2
2628 CD Delft

Referentie : 2017 – 171.
Betreft : Niet WMO-plichtig verklaring.
Protocol : RFID technologie.
METC-nr : **17 – 079**.

Vriendelijk verzoek bij alle correspondentie het METC-nr. te vermelden

Den Haag, 12 mei 2017.

Geachte mevrouw Meeuwsen ,

Het Dagelijks Bestuur van de Medisch Ethische Toetsingscommissie Zuidwest Holland, uitgebreid met 1 commissielid, heeft in haar vergadering van 10 mei 2017 het protocol besproken met de titel 'Automatische fase-detectie van operaties door het volgen van medische instrumenten binnen de OK met RFID-technologie'.
Dit onderzoek gaat u uitvoeren in samenwerking met dr. M. van der Elst, chirurg RdGG.

Het bovenvermelde protocol valt niet onder de reikwijdte van de Wet Medisch-wetenschappelijk Onderzoek met mensen (WMO).
Voor een dergelijk onderzoek is geen positief oordeel van een METC nodig.

Dit besluit is gebaseerd op de volgende documenten:
- Aanbiedingsemail van mw. F. Meeuwsen, PhD cabndidate TU Delft, d.d. 25 april 2017;
- Vragenlijst ter bepaling van de WMO plicht, ingevuld door mw. F. Meeuwsen, d.d. 25 april 2017;
- Onderzoeksprotocol, versie IV, d.d. 25 april 2017;
- TEP protocol.

Een kopie van deze verklaring zal aan de Directie van Reinier de Graaf Gasthuis worden gezonden

METC Zuidwest Holland

Namens de Medisch Ethische Toetsingscommissie Zuidwest Holland,

hoogachtend,

Mw. mr. M. Kirkels-Breukers,
secretaris

Sportlaan 600 2566 MJ Den Haag tel: 070 210 7680 metczwh@hagaziekenhuis.nl www.metczwh.nl

A.2. Research protocol

ONDERZOEKSPROTOCOL

Titel	*Automatische fase-detectie van operaties door het volgen van medische instrumenten binnen de OK met RFID-technologie.*
Versie	*V1*
Datum	*25/04/2017*
Project coördinator	*John van den Dobbelsteen, associate professor* *Dept. of Biomechanical Engineering, faculty of Mechanical, Maritime and Materials Engineering, TU Delft* *Mekelweg 2, 2628 CD Delft*
Hoofdonderzoeker/ uitvoerder	*Frédérique Meeuwsen, PhD student* *Dept. of Biomechanical Engineering, faculty of Mechanical, Maritime and Materials Engineering, TU Delft* *Mekelweg 2, 2628 CD Delft*
Contactpersoon/expert RdGG	*Maarten van der Elst, chirurg* *RDGG, Afdeling Heelkunde* *Reinier de Graafweg 5, 2625 AD Delft*
Subsidieverstrekker	*DSW*

PROTOCOL HANDTEKENINGEN OVERZICHT

Naam	Handtekening	Datum
Project coördinator *John van den Dobbelsteen, associate professor.*	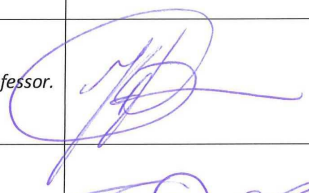	**25/04/2017**
Hoofdonderzoeker/uitvoerder: *Frédérique Meeuwsen, PhD student.*		**25/04/2017**
Contactpersoon/expert RdGG *Maarten van der Elst, chirurg*		**25/04/2017**

INHOUDSOPGAVE

SAMENVATTING

Motivatie: In dit onderzoek zullen individuele medische instrumenten uitgerust worden met radio-frequency identification (RFID) tags, om de locatie van de instrumenten te kunnen volgen binnen de OK. Uit deze informatie kan afgeleid worden of het medisch instrument in gebruik is door de chirurg. Deze technologie zal ingezet worden bij TEP operaties.

Doelstelling: 1.Fase herkenning van de procedure. 2. Herkenning van het werkpatroon van de operateur.

Onderzoeksopzet: Een pilot-study. Observationele cohort studie.

Studiepopulatie: de artsen die TEP procedures uitvoeren bij het Reinier de Graaf ziekenhuis te Delft

Belangrijkste studie parameters: Het voornaamste studiedoel is om de locaties van de instrumenten gedurende een operatie te volgen. Aan de hand van de locaties hopen we informatie over de voortgang te kunnen verkrijgen. Tevens geeft dit ons een indicatie wat de werkwijze van de operateur is.

Aard en omvang van de risico's verbonden aan deelname: Ons inziens zullen de risico's minimaal zijn. Onze studiepopulatie hoeft geen andere handelingen te verrichten dan het uitvoeren van een normale TEP procedure. Wij nemen geen vragenlijsten af.

De veiligheid van de aangepaste instrumenten is gewaarborgd door de instrumentenmakers van het Reinier de Graaf ziekenhuis. Mocht er zich toch iets voordoen met de instrumenten is er een extra set van originele instrumenten beschikbaar.

1. INTRODUCTIE EN MOTIVATIE

Dankzij de rijzende kosten van de gezondheidszorg is er in de afgelopen decennia steeds meer aandacht gekomen voor kostenefficiëntie binnen ziekenhuizen. De operatiekamer (OK) is hierin een van de meest kostbare en complexe systemen en daarom een natuurlijk punt van aandacht. Effectief gebruik van de OK wordt gelimiteerd door de precisie waarmee operaties ingepland kunnen worden en een nauwkeurige inschatting van operatieduur is hierbij noodzakelijk. Gezien de inherente variabiliteit van operaties, is een daadwerkelijk goede inschatting gebaseerd op live informatie uit de OK.

In dit onderzoek zullen individuele medische instrumenten uitgerust worden met radio-frequency identification (RFID) tags, om de locatie van de instrumenten te kunnen volgen binnen de OK. Uit deze informatie kan afgeleid worden of het medisch instrument in gebruik is door de chirurg. De vervolgstap is om vanuit instrumentgebruik de huidige fase en daarmee de voortgang van de operatie te voorspellen, met als uiteindelijk doel de efficiëntie te verbeteren.
Tevens hopen we meer inzicht te krijgen in het specifieke instrumentgebruik en werkpatroon van de operateurs.

2. DOELEN

Hoofddoel:
Het **doel** van het onderzoek is hiermee tweeledig:

1. Aantonen dat data van instrumentgebruik tijdens operaties gebruikt kan worden om de fase (en daarmee resterende duur) van operaties te voorspellen.

2. De werkwijze van een operateur te herkennen aan de hand het gebruik van de instrumenten gedurende een operatie.

3. ONDERZOEKSOPZET EN STUDIEPOPULATIE

Dit onderzoek is een pilot-studie, die zo veel mogelijk volgens regels van een observationele cohort studie zal worden uitgevoerd. Ons streven is een groep van 50 TEP procedures te meten. De geschatte onderzoeksduur is zes maanden. Er zal niet gerandomiseerd worden.
De studiepopulatie is de artsengroep van het RDGG die TEP operaties uitvoert.

In principe kunnen alle geplande procedures in het Reinier de Graaf ziekenhuis gemeten worden. Exclusiecriteria zijn niet van toepassing, aangezien deze operatie een redelijk standaard executie kent.

4. METHODEN

4.1 Studie parameters

4.1.1 Primair doel

Herkenning van de verschillende fases van de operatie.

4.1.2 Secundair doel

Herkenning van het werkpatroon van de operateurs.

4.2 Studie procedures

Alle instrumenten die gebruikt worden tijdens een TEP procedure worden van een RFID tags voorzien. Op de overzettafel wordt een RFID scanner geplaatst, onder de steriele doeken. Op deze manier kan gelezen worden wanneer de instrumenten in gebruik zijn. Er wordt van de operateurs geen andere handelingen verwacht, dan hun gebruikelijke manier van opereren. Ook zullen de tags en scanner het gebruikelijke werkproces niet verstoren.
De instrumenten worden voorzien van een RFID tag door Van Straten Medical (Edisonbaan 20, 3439 MN, Nieuwegein, www.vanstratenmedical.com). De scanners en de software om de data op te slaan komt van Bexter (Papsouwselaan 119T 2624 AK Delft, www.bexter.nl).

Mochten er zich toch onvolkomenheden voordoen, dan is er een extra set met originele instrumenten (zonder RFID tags) beschikbaar om de operatie te vervolgen.

Er wordt in geen van de gevallen een relatie gelegd tussen het werkpatroon van de arts en de uitkomst/kwaliteit van de operatie.

5. VEILIGHEIDSRAPPORTAGE

5.1 Nadelige effecten

Wanneer er sprake is van enige nadelige effecten voor de voortgang van de operatie, is er een extra set instrumenten zonder RFID tags aanwezig. Hiermee kan de operatie zonder oponthoud vervolgd worden.

5.2 Data veiligheid

De verkregen data wordt geanonimiseerd opgeslagen door de hoofdonderzoeker. Tevens wordt er geen data van de patiënten opgeslagen.

6. ADMINISTRATIEVE ASPECTEN EN PUBLICATIE

6.1 Behandeling en opslag van data en documenten

Er wordt geen persoonlijke informatie over de patiënten geregistreerd. De data van het onderzoek worden opgeslagen op de server van de TU Delft.

6.2 Openbaarmaking en publicatie beleid

De verkregen data zijn bezit van de TU Delft. Publicatie wordt gedaan door F. C. Meeuwsen, in overleg met alle partijen.

B

Informed Consent

Instrumentengebruik registreren voor een effectievere operatiekamer planning

Geachte heer/mevrouw,

Wij vragen u om mee te doen aan een medisch-wetenschappelijk onderzoek. Meedoen is vrijwillig. Om mee te doen is wel uw schriftelijke toestemming nodig. U ontvangt deze brief omdat u binnenkort en TEP-ingreep ondergaat.

Voordat u beslist of u wilt meedoen aan dit onderzoek, krijgt u uitleg over wat het onderzoek inhoudt. Lees deze informatie rustig door en vraag de onderzoeker uitleg als u vragen heeft. U kunt ook de onafhankelijk deskundige, die aan het eind van deze brief genoemd wordt, om aanvullende informatie vragen. U kunt er ook over praten met uw partner, vrienden of familie.

Onderzoeksteam:
Frédérique Meeuwsen
PhD kandidaat, Technische Universiteit Delft

Jeroen Koffeman
Master student, Technische Universiteit Delft

Maarten van der Elst
Chirurg, Reinier de Graaf ziekenhuis

Deze toestemmingsverklaring bestaat uit twee delen:

- **Informatie over ons onderzoek**
- **Toestemmingsverklaring, welke ondertekend moet worden als u beslist om te participeren aan het onderzoek**

U zult een kopie meekrijgen van de volledige toestemmingsverklaring.

Deel 1: Informatie

1. Algemene informatie
Dit onderzoek wordt uitgevoerd door de Technische Universiteit Delft, in samenwerking met het Reinier de Graaf ziekenhuis.

2. Doel van het onderzoek
In dit onderzoek wordt de bruikbaarheid getest van informatie over het instrumentengebruik tijdens operaties.

3. Achtergrond van het onderzoek
De complexiteit van operaties zorgt vaak voor vertragingen van ingrepen. Deze vertragingen leiden vaak tot inefficiënte OK-planningen. Er wordt onderzoek gedaan naar systemen die de fases van operaties automatisch kunnen herkennen. Het automatisch bijhouden van deze fases levert bruikbare informatie voor de OK-planners, waardoor er efficiënter gepland kan worden. Het instrumentengebruik tijdens operaties kan bijdragen aan het herkennen van de verschillende fases. Het instrumentengebruik wordt gemeten met behulp van een antenne die tags kan lezen, welke bevestigd zijn aan de instrumenten.

4. Wat wordt er van u verwacht
U zult volgens de normale gang van zaken behandeld worden. Er zijn vanuit de patiënt en arts geen extra handelingen vereist om dit onderzoek te doen.

5. Mogelijke risico's
De testopstelling maakt gebruik van een antenne die radiogolven uitstraalt. Over het effect van radiogolven op omringende apparatuur op de operatiekamer is nog geen eenzijdige conclusie. Op de operatiekamer van het Reinier de Graaf ziekenhuis is de antenne op volledig vermogen getest. Bij deze test heeft er geen enkel omliggend apparaat storing vertoond. Tijdens de ingreep zal er continue een onderzoeker bij de antenne zitten om deze uit te schakelen wanneer een van de apparaten op de operatiekamer ongewoon gedrag vertoond.

6. Mogelijke voordelen en nadelen
U heeft zelf geen voordeel van meedoen aan dit onderzoek. Uw deelname kan wel bijdragen aan het verkrijgen van meer kennis en informatie over de bruikbaarheid van data over instrumentengebruik voor het ontwikkelen van een effectievere OK-planning.

7. Als u niet wilt meedoen of wilt stoppen met het onderzoek
U beslist zelf of u meedoet aan het onderzoek. Deelname is vrijwillig. Als u niet wilt meedoen, wordt u op de gebruikelijke manier behandeld.

Als u wel meedoet, kunt u zich altijd bedenken en toch stoppen. Ook dan wordt u weer behandeld op de gebruikelijke manier. U hoeft geen reden van stoppen te geven. Wel moet u dit direct melden aan de onderzoeker.

Als er nieuwe informatie over het onderzoek is die belangrijk voor u is, laat de onderzoeker dit aan u weten. U wordt dan gevraagd of u blijft meedoen.

8. Gebruiken bewaren van uw gegevens

Voor dit onderzoek worden uw persoonsgegevens **niet** verzameld, gebruikt en bewaard. Voor het onderzoek is alleen de data over het gebruik van de instrumenten tijdens de operatie van belang. Deze data kan in geen enkel opzicht herleid worden naar uw persoonsgegevens. De data zal **wél** beschikbaar zijn voor studenten van de Technische Universiteit Delft.

Tijdens de test zullen foto-opnames gemaakt worden, ten behoeve van analyse, wetenschappelijke presentaties en publicatie doeleinden. Op deze foto-opnames bent u als patiënt **niet** identificeerbaar. Voor het onderzoek wordt uw toestemming gevraagd om de foto-opnames te maken tijdens uw behandeling. Let op, dit is optioneel en dus niet verplicht om aan het onderzoek mee te kunnen doen.

9. Heeft u vragen?

Bij vragen kunt u contact opnemen met het onderzoeksteam.

Deel 2: Toestemmingsverklaring:

- Ik heb het informatiegedeelte gelezen, of deze is aan mij voorgelezen. Ik heb vragen kunnen stellen, welke voldoende beantwoord zijn. Ik had genoeg tijd om te beslissen of ik meedoe aan het onderzoek.

- Ik weet dat meedoen vrijwillig is. Ook weet ik dat ik op ieder moment kan beslissen om toch niet mee te doen of te stoppen met het onderzoek. Daarvoor hoef ik geen reden te geven.

- Ik geef □ **wel**
  □ **geen**
  Toestemming om anonieme foto-opnames van de ingreep vrij te geven voor het onderzoeksteam.

- Ik wil meedoen aan dit onderzoek.

Naam proefpersoon:

Handtekening: Datum : __ / __ / __

Ik verklaar dat ik deze proefpersoon volledig heb geïnformeerd over het genoemde onderzoek.

Als er tijdens het onderzoek informatie bekend wordt die de toestemming van de proefpersoon zou kunnen beïnvloeden, dan breng ik hem/haar daarvan tijdig op de hoogte.

Naam onderzoeker:

Handtekening: Datum: __ / __ / __

C

Feature Engineering

An single entry from the manually annotated data does not provided sufficient information to train a Random Forest model. Therefore, a selection of Features is introduced, see Table C.1. The features originate from the research that is done by [2]. The elaboration on the different features is cited, and adapted from [2]:"From the binary instrument usage vectors from the start of the procedure until the current time (t) the cumulative usage up until s derived. As the instrument usage is discretized with a time step of one second, the cumulative usage is given by the sum of the vector from time 1 to t. Furthermore, by checking whether the cumulative usage is larger than zero, it is noted whether the instrument has been used during the current procedure. Another set of features encodes changes in the use of the instruments. The backward difference of a signal $Instrument$ is given by $Instrument(t) - Instrument(t-1)$. For the binary instrument usage signals, the backward difference takes a value of either 0 (no change), +1 (instrument now in use) or -1 (instrument not in use anymore). By choosing different time lags (1 second, 1 minute, 5 minutes, 10 minutes) the usage history of the instrument is taken into account. Epochs of instrument use describe the sessions of consecutive use of an instrument. These can be found by counting the times when the backward difference of the instrument with a one-sample delay is equal to one. Finally several summarizing features are derived. By summing the instrument vectors at time, we obtain the total number of instruments currently in use. Similarly, by summing over the usage indicators, we obtain the total number of different instruments that have been used in the current procedure. A total of 91 features are generated for every time step and appended to the time-based log."

Table C.1: Table copied and adapted from [2]. Description of 92 features used for the classification model. Instrument refers to one of the 11 tagged instruments (Table 2.2). `Instrument[t]` takes value 1 when instrument is in use at time `t` or 0 when not in use.

Feature	**Description**	**Count**	**Type**	**Matlab implementation (at time t)**
Surgical time	Elapsed time since surgery onset, in seconds	1	Integer	`t`
Instrument	Instrument currently in use	11	Binary	`Instrument(t)`
InstrumentCTL	Cumulative used time of instrument in this procedure	11	Integer	`cumsum(Instrument)`
InstrumentUsed	Instrument used in current procedure	11	Integer	`cumsum(Instrument) > 0`
InstrumentD1, ..., InstrumentD600	Backward difference per instrument with delay of 1, 60, 300 and 600 seconds	44	Categorical (-1,0,1)	`Instrument(t) - Instrument(t-Delay)`
InstrumentE	Epochs of use per instrument	11	Integer	`Instrument(t) - Instrument(t-Delay)`
numInstruments	Total number of instruments currently in use	1	Integer	`sum(Instrument1(t) + .. + InstrumentN(t))`
numInstruments-Used	Total different instruments used in this procedure	1	Integer	

D

Raw data from the pilot study

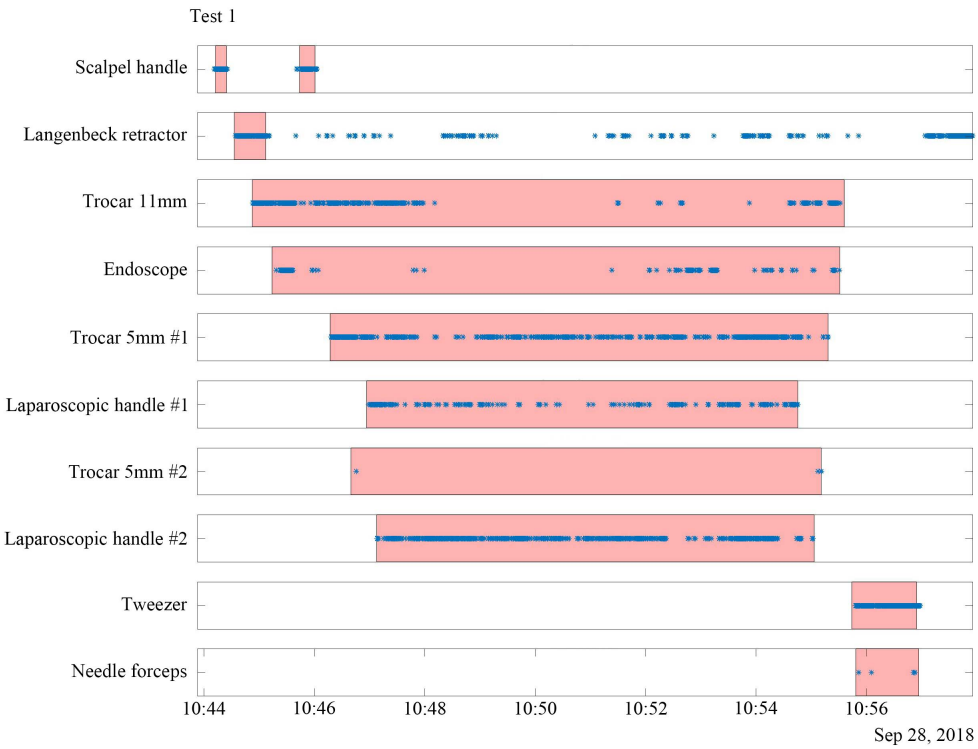

Figure D.1: Raw data of first test during the pilot study.

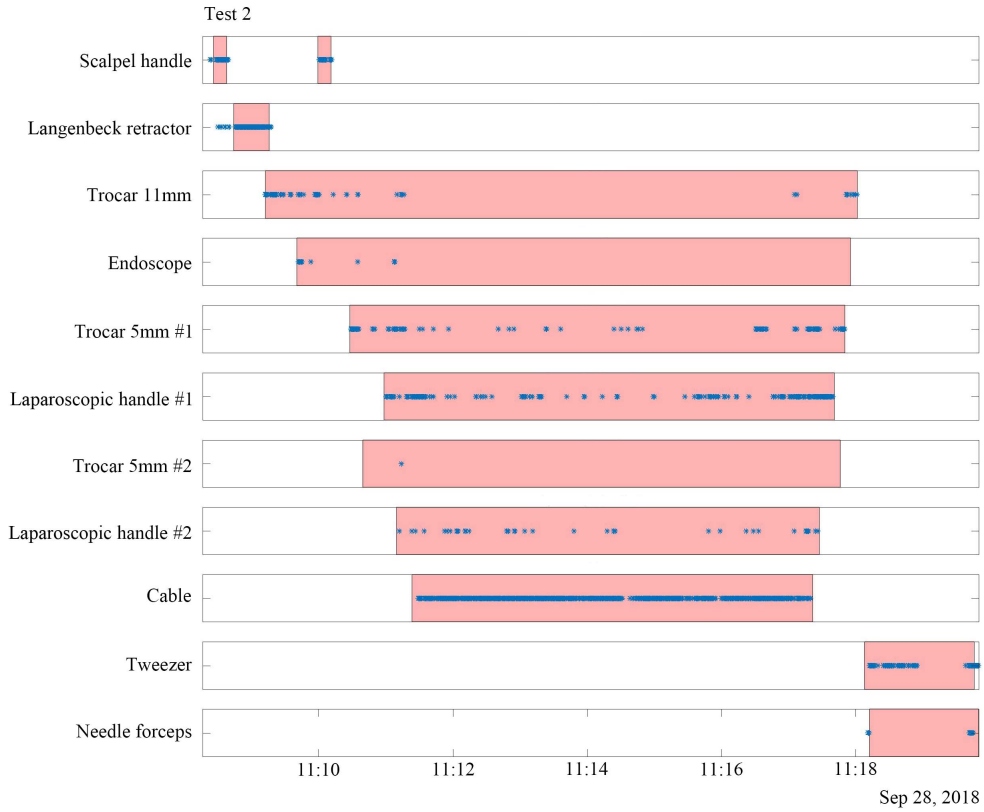

Figure D.2: Raw data of second test during the pilot study.

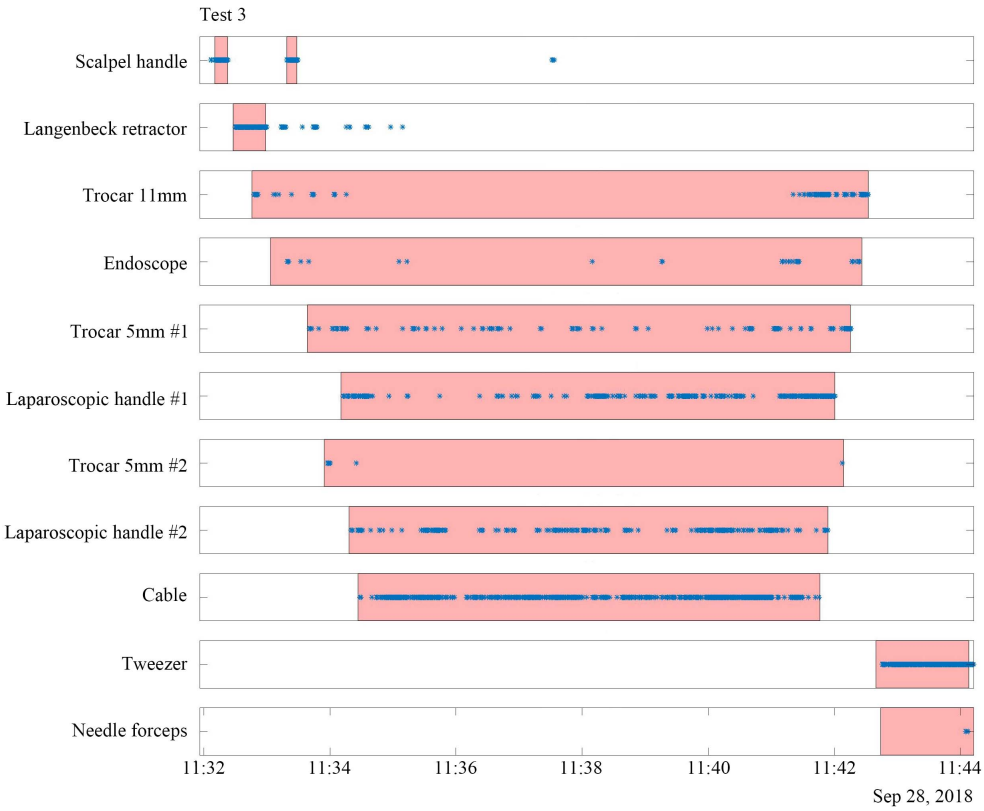

Figure D.3: Raw data of third test during the pilot study.

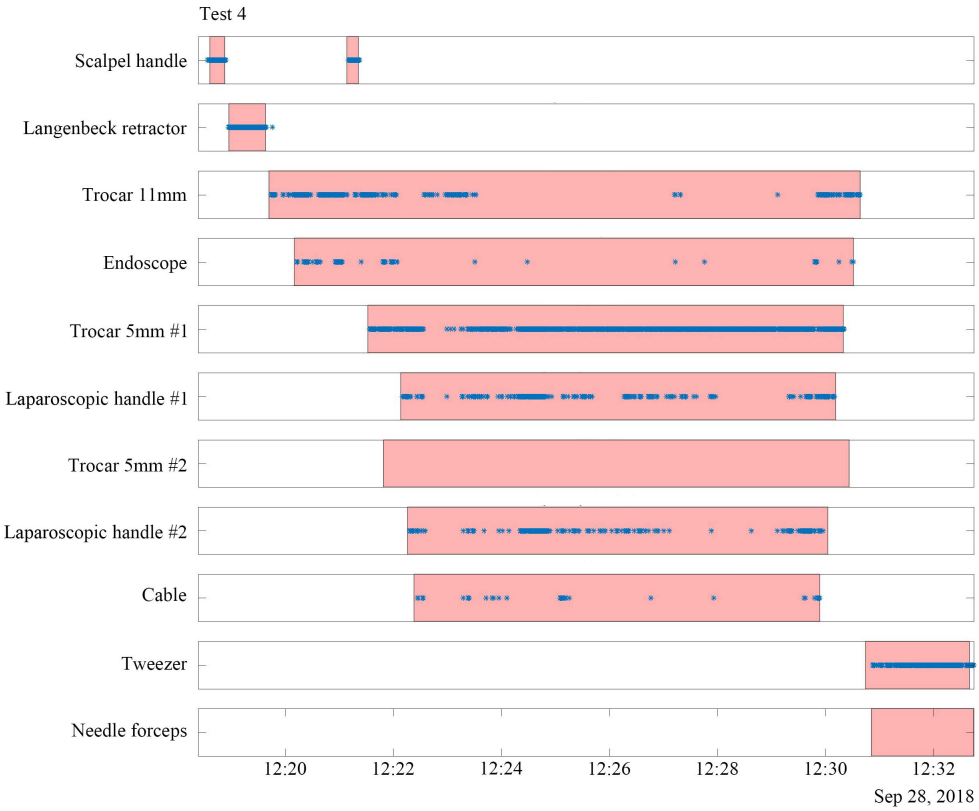

Figure D.4: Raw data of fourth test during the pilot study.

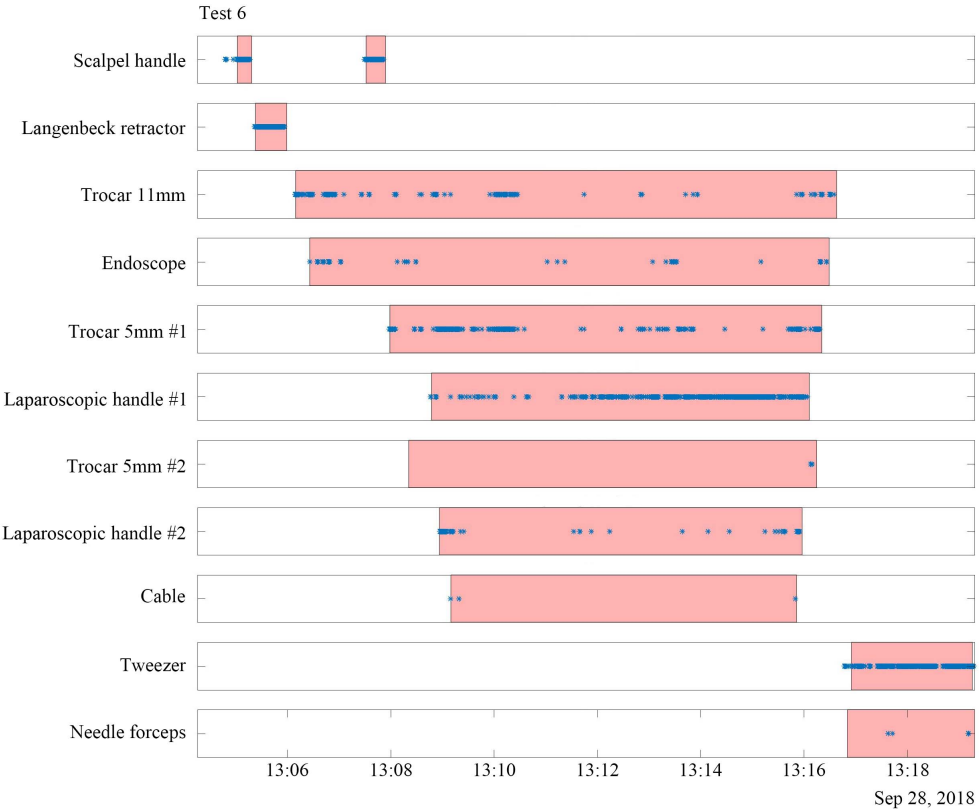

Figure D.5: Raw data of sixth test during the pilot study.

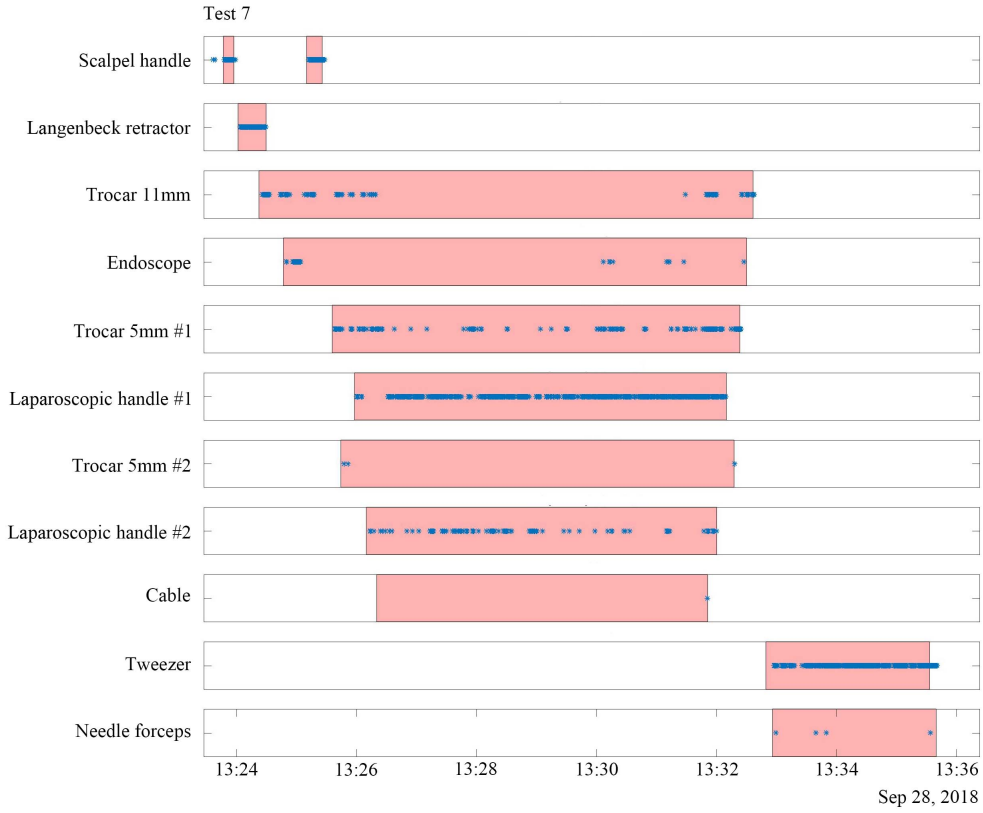

Figure D.6: Raw data of seventh test during the pilot study.

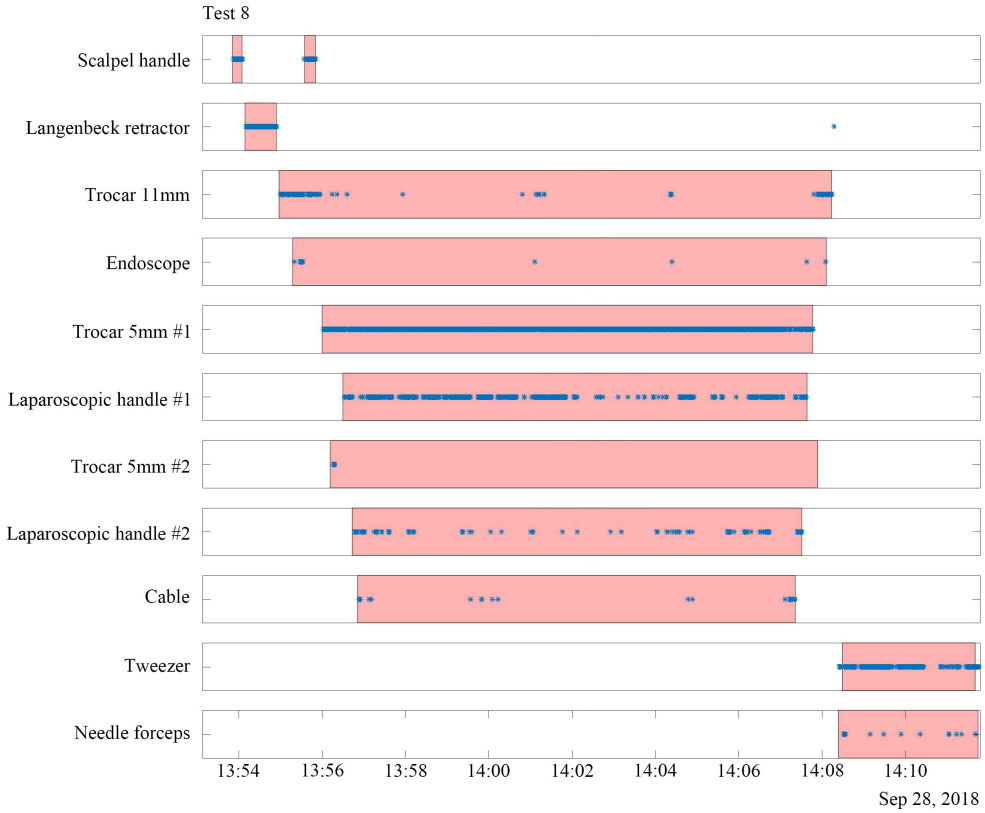

Figure D.7: Raw data of eighth test during the pilot study.

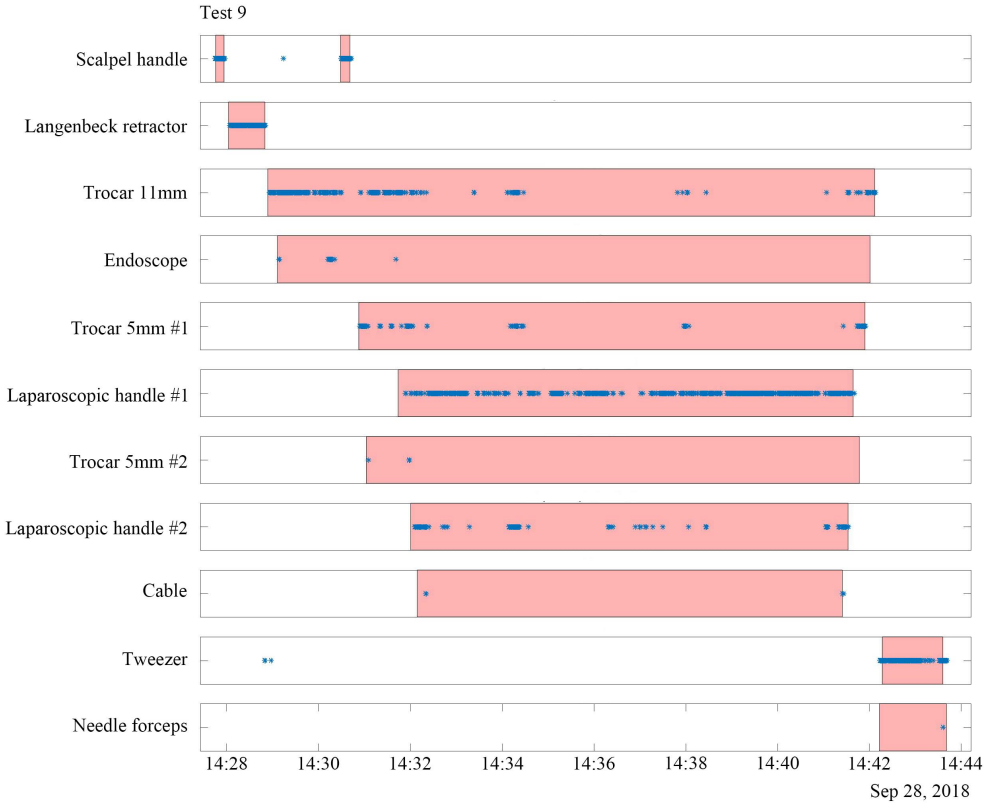

Figure D.8: Raw data of ninth test during the pilot study.

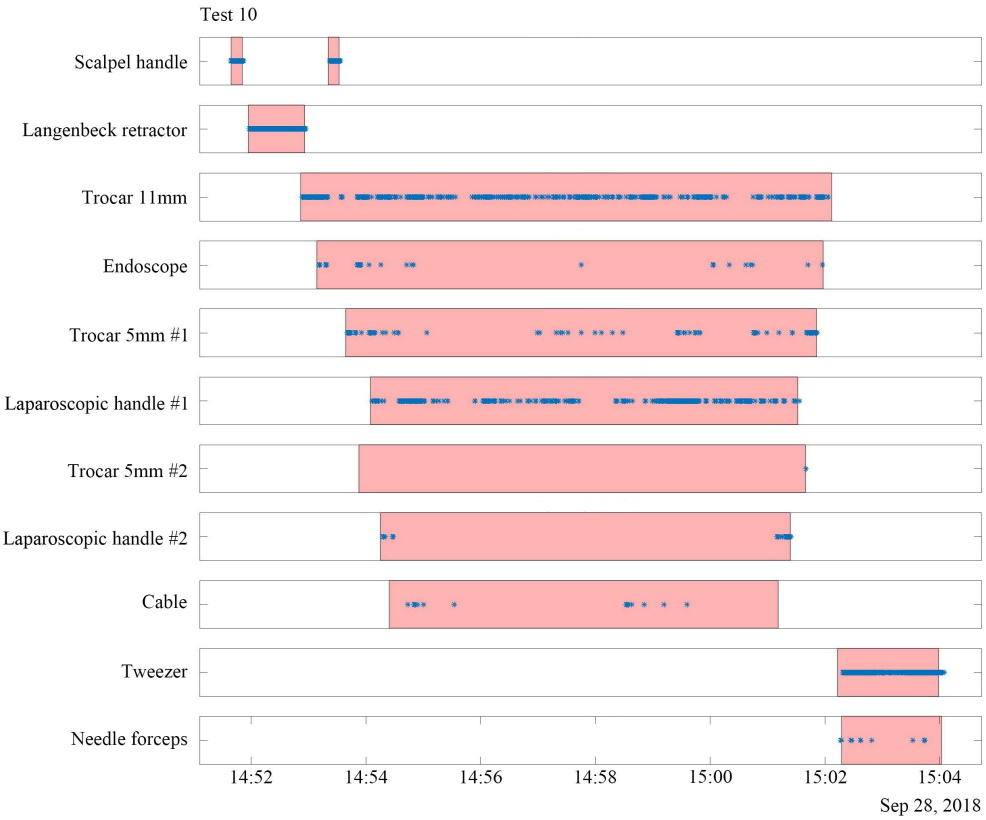

Figure D.9: Raw data of tenth test during the pilot study.

E

Proposed setup for strength test

This appendix presents a proposal for a setup to test the strength of the designed attachment (Part II). The strength is evaluated by means of a controlled impact to simulate a drop on the floor. The level of impact is determined by the worst case scenario where the instrument with the greatest mass drops from 1.5 meters on the ground. In order to mimic a drop of the instrument in a controlled environment, the potential energy from a drop is considered equal to the potential energy of a mass M connected to a thread in a pendulum setup (Figure E.1), where the specimen refers to the designed attachment:

$$PE_{drop} = PE_{pendulum} \tag{E.1}$$

which results in

$$m * h = M * L * (1 - \cos(\theta)) \tag{E.2}$$

Where m is the mass of the instrument, h is the drop height (1.5 meters), M is the mass connected to the thread of the pendulum, L is the length of the thread, and θ is angle between the thread and the vertical axis. In this experiment, both the mass of the thread and friction are neglected. The constructional elements of the setup are considered rigid and the specimen is assumed to be in a fixed position.

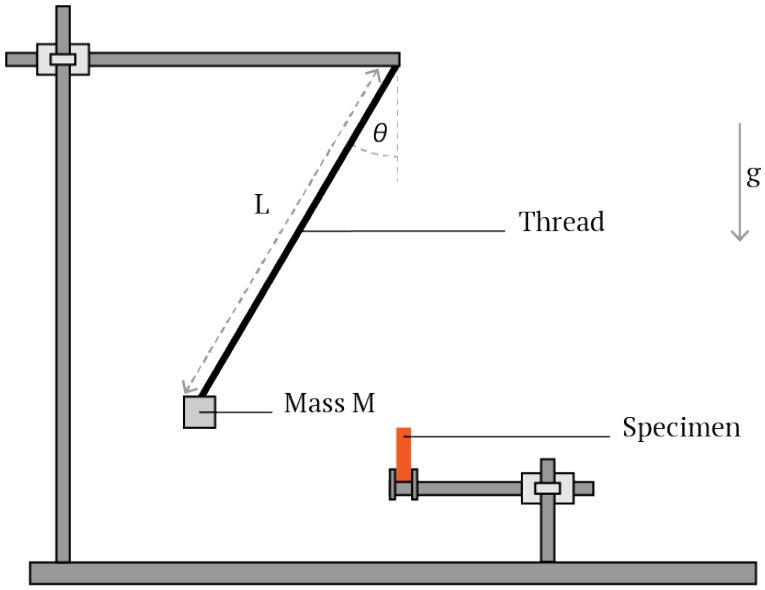

Figure E.1: Schematic pendulum setup for impact test of the epoxy.

F

Real time phase recognition

F.1. Introduction

As shown in this thesis, intraoperative data can be acquired through instrument identification using RFID-technology. The aim of such data acquisition is to eventually provide the OR-schedulers with feedback about the progress of ongoing surgeries. This Appendix elaborates on preliminary work to research the possibilities of converting the intraoperative data from the RFID-system to a phase prediction in real time. Basically, a script is required that can communicate with the RFID-reader during surgery. The data that is communicated with the reader must be converted in such a way that it can be parsed to the Random Forest model, which in turn estimates the phase.

F.2. Method

The data traffic between the reader and the laptop occurs via ethernet, using the IPv4 protocol. Fortunately, this traffic can be captured and decoded using a network protocol analyzer. In this case, the application Wireshark [44] is used to run a live capture of the data that is transferred over ethernet. The Python module PyShark [45] allows parsing data from a live Wireshark capture into a Python script for further processing. The structure of the written Python script is as following: Two threads run simultaneously during an ongoing surgery. The first thread fills a buffer with data from Wireshark using the PyShark module for a fixed time of one second. After one second, the data in the buffer is processed in such a way that it results in a list of all tag id's that are detected. The list of tag id's is parsed to the second thread, after which the buffer is cleared and re-filled again. The list of detected tag id's is then simultaneously transformed by the second thread into a time-based entry as presented in Table 2.7. After Feature Engineering (Section C), the time-based entry is parsed to the Random Forest model to estimate the current phase. The resulting phase is printed to the user interface of the OR-schedulers.

F.3. Results and Discussion

The communication between the Python script and the Wireshark application functions properly. Also, the rest of the Python script appears to function correctly. However, a complete test could not be performed within the timeframe of this study. The Random Forest model is namely generated based on the instrument usage during a TEP-procedure. A complete test, that includes the detection of instruments by the antenna thus requires the tagged instruments that are used during this study. These instruments were unfortunately stored at Combi-ster and thus not available for testing. Such a real time phase recognition program can be combined with a script that estimates the remaining duration of surgeries, as proposed by [2].